UNIVERSITÀ
DEGLI STUDI
DI PADOVA

UNIVERSITY OF PADUA

DEPARTMENT OF INDUSTRIAL ENGINEERING

MASTER DEGREE IN CHEMICAL ENGINEERING AND INDUSTRIAL PROCESSES

Master Thesis in
Chemical Engineering and Industrial Processes

Iono- and Hydrothermal synthesis and characterization of Ca-Mn Oxide catalysts for water-splitting

Supervisors: Prof. Paolo Canu, Prof. Jyri-Pekka Mikkola

Tutors: Dr. Hasna Bourajoini, Dr. Santosh Khokarale

Graduand: SACHA ROSSETTO

ACADEMIC YEAR 2015-2016

Abstract

In this thesis, research aiming at an efficient Manganese based catalyst was carried out on the water splitting reaction. More specifically, different preparation methods and different types of ionic liquids as solvent, template and structural agent were investigated in order to study their influence and understand how the strong ionic interactions have an influence in the surface area of the resulting material.

Following the synthesis, each catalyst was measured for its activity mainly by the use of three techniques: Clark Electrode, Gas-Chromatography and the CV/LSV analysis (Cyclic Voltammetry/Linear and linear sweep voltammetry). Also characterization studies were carried out in terms of different aspects through analysis like SEM, ICP-OES, Raman spectroscopy, BET, XRD and XPS in order to understand the morphology of materials, determine the amount of elements of which it is made, analysis of the crystal structure, measurement of the surface area/composition and determination of the manganese oxidation state (fundamental characteristic of catalysts for this kind of reaction). Furthermore, after choosing the compound with the best catalytic activity, reaction kinetics was analysed and the role of CaMnOx in terms of the reaction mechanism of the reaction was speculated about.

At the end of this study it has been pointed out several information regarding for example the optimal synthesis parameters and operative conditions, the important role of Calcium, more than any other alkaline earth metal, and the advantages that ionic liquids give to the final product and during the synthesis process.

It may therefore seem, that there exists a real possibility in a near future to utilize this catalyst in an industrial way, for large-scale production of hydrogen and oxygen. However, in order to reach this aim, there is still a lot to do. Conversion and yield are still low and the open debate about mechanism and role of the “oxidation agent’’ in the water splitting reaction hasn’t been solved yet.

Contents

Introduction

The environment care is one of the most important topic for the modern human civilization, and the consume of energy from fossil fuel is probably the main cause of pollution and green-house gases production. For this reason, the research of a new renewable energy source for the world sustenance (opposite from fossil fuel), nowadays, has received great attention. In this way, science had achieved many discoveries: from the use of solar panels for water heating or the production of electricity to the use of the latter in automotive branch rather than research on new kind of fuels.

A new aim in these years is to engineer an artificial way to mimic what the nature performs in every vegetal species: the photosynthesis process. Based on that process, plants are able to carry out water splitting through which they produce oxygen (from water splitting) or by means of following reactions other organic products (e.g. carbohydrate). The success of this research could bring forth an excellent alternative to the fossil fuels. In fact, to date, one of the most important factors hindering the use of hydrogen as an alternative fuel to oil, is the lack of an efficient process (economically and energetically advantageous) for its production that is independent of petrochemical ones. Furthermore, the water splitting reaction could be used in the field of solar energy, substituting common electricity storing systems with a chemical storing system that contemplate the hydrogen production and following, the use of this ‘’solar fuel’’ in the electricity production (e.g. by means of a turbine).

In natural photosynthesis, oxidation of water takes place at the oxygen evolving complex of Photosystem II, which is comprised of an inorganic manganese based cluster surrounded by functionally important protein ligands. The structure described here (Mn_4O_5Ca) is responsible for the transfer of four electrons and four protons, as well as for the O-O bonding which readily oxidizes water into O_2. This study, will be focused on developing calcium and manganese oxides using different ionic liquids in the view of mimicking a synthetic inorganic water oxidation catalyst similar to that of the CaMn-oxide cluster in Photosystem II for the water oxidation reaction.

This report will be structured in four chapters. In the first one, it will be given an overview of all what concerns the water splitting and synthesis of water splitting catalysts (mechanism, oxidant agents, Iono- and Hydrothermal synthesis), while in the next ones a traditional scientific reporting scheme is followed that consists of a material and method description, an experimental part where all the results obtain will be shown, elaborated and discussed. Finally, this thesis concludes at the end with final observations and future suggestions in order to identify the right path to obtain considerable improvements in this field.

This thesis reports what has been done in five months of research during the Erasmus period carried out at the Umeå University, Sweden, at the Department of Chemistry residing in the KBC-Huset under the supervision of Prof. Dr. Jyri-Pekka "J-P" Mikkola, Phd student Hasna Bourajoini and Dr. Santosh Khokarale, in collaboration with the University of Padua under the supervision of Prof. Paolo Canu.

Chapter 1

General concepts

In the world of chemicals, the word catalysis takes on a really important role. It is estimated that the ~90% of the industrial reaction are catalysed [1]. This means that the studies on the synthesis and optimization of their characteristic proprieties (surface area, turnover number, type of porosity, life-time, production cost etc…) are essential to reach a sensible improvement of existing processes but also to discover new potential ones.

One of the most interesting reactions that we are not still able to carry out (in an efficient way) is the water splitting reaction (see Eqs. 1.1, 1.2 and 1.3).

$$2\ H_2O \rightarrow 2\ H_2 + O_2 \qquad (1.1)$$

$$4\ H^+ + 4\ e^- \rightarrow 2\ H_2 \qquad (1.2)$$

$$2\ H_2O \rightarrow O_2 + 4\ H^+ + 4\ e^- \qquad (1.3)$$

where Equation 1.1 represent the total reaction while Equation 1.2 and Equation 1.3 stand for the reduction and oxidation steps, respectively.

Useful in many applications, hydrogen is currently produced mainly from processes that make use of fossil fuels (particularly natural gas). Anyway, this process, unlike the classical pathways, is characterized by:

- a green reaction;
- it does not lead to formation of by-products (oxygen in fact, having a high market value, is not considered as such);
- the reagent (water) is one of the most abundant on the earth and it is not harmful for health;

On the other hand, water splitting reaction is unfortunately thermodynamically and kinetically disadvantaged and, therefore, needs to be catalysed as happens in every

vegetal species (ΔG=56.62Kcal/mol$_{H_2O}$, ΔH=68.315Kcal/mol$_{H_2O}$ at 300K and atmospheric pressure). In particular, the rate determining step regards the water oxidation half-reaction.

In these years, the research has proposed various catalysts to perform the water splitting (for example based on metals oxides of iron, copper, nickel, cobalt, ruthenium) and even if the last two have shown an appreciable activity, they are too rare and too expensive to consider them as the ‘’final solution ‘’.

In nature, inside chloroplasts, a complex called OEC (or water-oxidising complex, WOC), following the mechanism PSII, splits the molecules of water in hydrogen and oxygen by means of the sunlight. Recently, it has been discovered that the aforementioned OEC complex would have been constituted by a structure mainly formed by a $CaMn_4O_5$ complex (see Figure 1.1) closely bound to its highly conserved amino acid environment. The metal ions are interconnected by μ-oxido ligands, with three Mn and one Ca forming a distorted $CaMn_3O_4$ cubane. The fourth manganese ion is then bound to this moiety by additional μ-oxido ligands. This new structural information represents an enormous progress in PSII research [2].

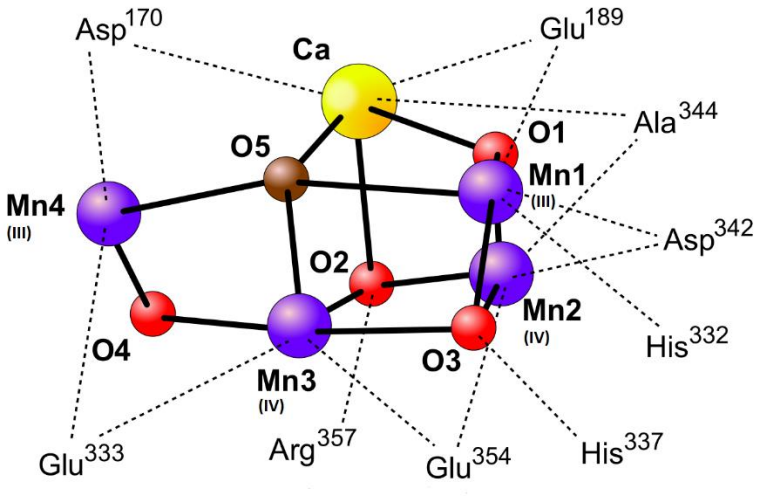

Figure 1.1 *Oxygen Evolving Complex structure. Adapted from* [3].

Here originates the interest for CaMnOx as catalyst in the water-oxidation reaction; in fact:

i. a manganese centre actually catalyses water oxidation in PS II with incomparable efficiency;

ii. manganese complexes are known for all oxidation states between Mn^{II} and Mn^{V}, thereby making multiple one-electron oxidation processes possible;

iii. manganese is a cheap and abundant metal and thus potential future applications on a large scale are feasible[4].

1.1 Oxidation mechanism of the half-reaction inside the OEC complex

Studies on the OEC complex are unfortunately still very few since the interest for this bio-chemical process arose relatively recently. After the first fundamental step as the ‘’natural’’ catalyst composition (mainly $CaMn_4O_5$ surrounded by different type of amino acids that have the function of coordinating agents) that was discovered, science is attempting to unveil the ensemble of steps pathway that results in the oxygen molecule evolution, starting from two molecules of water. However, the exact mechanism of water-oxidation catalysis by the OEC is still not known. Nevertheless, it is clear today that the $CaMn_4O_5$ complex is oxidised stepwise in single-electron steps during the water-oxidation reaction, cycling through five individual oxidation states (see Figure 1.2). Oxidizing equivalents are stored in the $CaMn_4O_5$ complex mainly through Mn-centred oxidations as the manganese ions are oxidized from Mn^{III} to Mn^{IV} [2,5–8]. For the highest oxidation state of the OEC (known as S4), the oxidation of an oxido ligand (O^{-II}) to its oxyl radical form (O^{-I}) has been suggested [2,9].

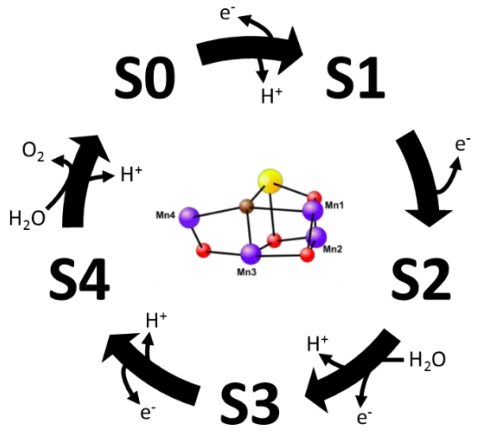

Figure 1.2 *Mechanism of reaction, that thanks to five transitions of Manganese oxidation state, allows following a multiple steps pathway with lower activation energy than single step. This mechanism is called Kok cycle (the catalytic cycle of the water oxidation). Water-binding within the cycle is based on FTIR data by Noguchi. Both waters likely represent ones that become substrates in the next cycle* [10,11]. *Image adapted from* [12].

In the S0→S1, S1→S2, S2→S3, and S3→S4 transitions, light (E=hν) is used to oxidize a chlorophyll molecule, which in turn oxidizes the OEC via a redox-active tyrosine. Only, the S4→S0 transition is light independent [13].

1.2 Role of Calcium

Ca^{2+} has been identified as an essential cofactor in the OEC in PSII reaction and the Ca^{2+}-binding sites in PSII have been previously studied by several methods [13–22]. Sr^{2+} is the only cation that can functionally substitute for Ca^{2+} in the OEC [19,23,24]. In the early proposals for the mechanisms of oxygen evolution by the OEC in PSII, there was no roles for calcium [25]. However, recent data supports the hypothesis that calcium, indeed, has an important role [26] and some mechanisms are proposed regarding the role of calcium in oxygen evolution reaction. Pecoraro and co-workers proposed that a terminal Mn(V)═O undergoes a nucleophilic attack by a Ca^{2+} bound hydroxide ligand to form a Mn-bound hydroperoxide [27]. Brudvig and co-workers have also proposed a mechanism in which a Ca^{2+} ion plays a role as a weak Lewis acid. In the mechanism, a water bound to calcium reacts with a Mn(V)═O species to form the O─O bond through a nucleophilic attack [28]. The idea has been elaborated by Brudvig and co-workers to generate a mechanism that accounts for the detailed of oxygen evolution by PSII [29].

A number of experiments demonstrate the role of calcium in the assembly and stability of the OEC [26]. Analogous to the role of calcium in oxygen evolution reaction, calcium-manganese oxides could be proposed and tested via simple experiments. In addition to this role, calcium ions stabilize the high valence states of manganese, at high temperatures, in calcium-manganese oxides. Without calcium ions, only manganese (II) or (and) (III) are stable at 800°C or higher temperatures [30,31].

1.3 Ionic liquids

Over recent years, ionic liquids (ILs) have received great attention in many fields [32]. Most of the studies have focused on the ‘green’ chemistry [33] potential of these compounds, with particular emphasis on the drive to replace organic solvents in homogeneous catalysis [34]. The particular property of ILs that makes them

environmentally suitable for these purposes is their low vapour pressure [35], which brings along significant advantages when replacing highly volatile organic solvents. However, there are many other uses of ionic liquids in diverse areas of technology ranging from electrolytes in batteries and fuel cells [36], as electrodeposition solvents [37], to the use of supported ionic liquid as catalysts [38]. In some reactions (as the one introduced as the topic of this thesis) the ILs act only as inert solvents while in others the ILs play a more active role in the reactions that take place. Ionic liquid can be defined in a rough way to be considered as any material in the liquid state that consists predominantly of ionic species. Any ionic salt that can be made molten can therefore be classified as an ‘’ionic liquid’’, always assuming that the ionic components of the solid remain intact upon melting [39]. There are many examples in the literature of molten salts them being used as the medium in which inorganic materials have been prepared [39]. Usually, these synthetic procedures take place at highly elevated temperatures, producing dense phase solids [39]. In general such molten salt synthesis methods have been used as direct replacements for traditional solid state synthesis techniques [40].

However, the modern definition of ionic liquids tends to concentrate on those compounds that are liquid at relatively low temperatures and that contain organic components [41]. Room temperature ionic liquids (RTILs) are, as the name suggests, liquid at room temperature while near room temperature ionic liquids (nRTILs) are often defined as being liquid below a certain temperature, often 100°C, although this varies depending on the application envisaged for the liquids. For iono-thermal synthesis, nRTILs are often defined as being liquid below about 200°C, the temperatures traditionally used in hydrothermal synthesis[42]. In modern terms, the term ionic liquid is almost exclusively reserved for liquids that contain at least one organic ion [39]. Usually, these organic components tend to be large and often quite asymmetric. This feature contributes to their low melting points by making efficient packing in the solid state more difficult. Many ILs have good thermal stability enabling them to be used at elevated temperatures even if in the experimental section we will discover that for some ILs it is not like this.

Upon use of an ionic liquid as synthesis solvent, among many of the existing types, it has been seen that imidazolium ILs possess pre-organized structures through mainly

hydrogen bonds that induce structural directionality in opposition to classical salts in which the aggregates display mainly charge-ordering structures [43]. They form extended hydrogen bond and π–π stacking networks in the liquid state and are consequently highly structured; that is, they can be described as ‘‘supramolecular” fluids [43]. This structural organization of the imidazolium ILs can function as an ‘‘entropic driver” for spontaneous, well-defined, and extended ordering of nanostructures. Therefore, the unique combination of adaptability toward other molecules and phases associated with the strong H-bond-driven fluid structure renders the imidazolium ILs as ‘‘templates” for the formation of nanostructures. These ILs are suitable medium for the preparation and stabilization of transition-metal nanoparticles [43].

1.3.1 Iono- and Hydrothermal Synthesis

Broadly speaking, the synthesis of crystalline solid state materials (as metal oxides) can be split into two main groups: those where the synthesis reaction takes place in the solid state and those which take place in solution. The solid state method, usually requires rather high temperatures to overcome difficulties in transporting the reactants to the sites of the reaction. The high temperatures of solid state reactions also tend to provide routes to the thermodynamically more favoured phases in the systems of interest but in the other hand this aspect lead to an economic disadvantage (high heat duty required).

Transport in the liquid phase is obviously much easier than in solids, and synthesis require much lower temperatures (often less than 200°C). The archetype of this type of preparative technique is hydrothermal synthesis, where the reaction solvent is water [44]. The most common method of accomplishing hydrothermal synthesis is to seal the reactants inside Teflon-lined autoclaves so that there is also significant autogenous hydrothermal pressure produced, often up to 15 bar. The lower temperatures required for hydrothermal synthesis often lead to kinetic control of the products formed, and it is much easier to prepare metastable phases using this approach than it is using traditional solid state approaches [39].

Iono-thermal method differs from the Hydrothermal one only because the solvent is a mixture of water and ILs or even pure ionic liquid. The potential advantage of this approach is that the competition between the solvent and template for interaction with any growing solid is removed when both solvent and template are the same species [39].

Indeed, respect to other solvents (as water), ionic liquids have some advantages: (i) they have low interface tensions in spite of their polar features, resulting in a high nucleation rate (making it suitable for the synthesis of crystal structures); (ii) ionic liquids can form extended hydrogen bond systems in the liquid state and are therefore highly structured, and thus can further affect the structures of resulting products (of fundamental importance is to find or design the most suitable); and (iii) as a tuneable medium, ionic liquids are immiscible with a number of organic solvents and can provide a non-aqueous and polar alternative for two-phase systems [45]. Furthermore, an additional advantage of ILs is their potential to combine several cations and anions, thus making it possible to modify the ILs' properties according to the desired particular applications [46].

Finally, another feature that ILs owned (as solvent-template in the synthesis of nanoparticles) is the ability to support the formation of a high porosity materials.

For all the aforementioned reasons, the iono-thermal synthesis seems the most promising one for the construction of the catalyst potentially similar to that present in OEC complex.

1.4 Methods of reaction activation

Since we are studying just only the half-reaction, i.e. oxidation, we were interested in running and testing the catalytic activity of calcium manganese oxide in this reaction only. In order do that, it was necessary to introduce inside the reaction volume an agent that has the function to accept the electrons produced from the water oxidation that takes the role of an *''oxidant agent''*. In this way, by reducing itself, it is able to accept the electrons (keeping the electro-neutrality) however destined to the water-reduction for hydrogen production. Examples of oxidant agents are: hydrogen peroxide (H_2O_2),

tert-butyl hydroperoxide (TBHP), oxone (HSO_5^-), hypochlorite (ClO^-) or cerium ammonium nitrate ($Ce(NH_4)_2(NO_3)_6$).

Among all the oxidant agent existing, cerium ammonium nitrate seems to be the best option for obtain clear and reliable results from the activity analysis. The reasons are essentially two:

- it has a high oxidant power;
- differently from hydrogen peroxide, TBHP or others oxidant agents, Cerium ammonium nitrate doesn't release Oxygen during its decomposition. This aspect is of fundamental importance since, during activity test, we are going to measure the oxygen produced.

Instead, in the case of an interest to run the complete water splitting reaction by the mean of a heterogeneous catalyst, there are two main methods:

- **Photo-activation**; reaction is activated and controlled by means of a photo-sensitive chemical groups present in the catalyst structure that is able to collect the energy needed from the light.
- **Electrochemical-activation**; the energy of activation is given from an electric potential imposed between two electrode (electrolysis).

Chapter 2

Materials and methods

In this chapter it will be described how the project has been carried on, starting from the explanation of all synthesis and analysis procedures to the kind of methods used in order to obtain reliable results and characterize the most promising catalysts.

2.1 Synthesis: material and method

There are several different production methods of CaMnOx and everyone affect sensitively the morphologic/chemical structure and so, the activity of the final product. For this reason, it became really difficult to understand which is the best and which to choose.

However, this project started by choosing one of the most popular synthesis methods and sticking to it. In such a way, we were able to compare the results between different catalysts. Then, subsequently we tried to optimize the synthesis procedure for each compound produced. The methodology chosen, involves in a common procedure to synthesize the CaMnOx production called the ‘’precipitation method’’ (Figure 2.1).

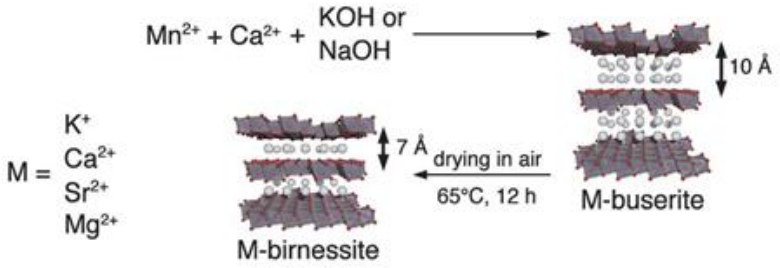

Figure 2.1 *Synthetic route for the preparation of M-birnessites. By variation of the initial metal ion concentrations, materials of different M/Mn ratios can be synthesised. The comproportionation reactions of* Mn^{2+} *under alkaline conditions initially result in the formation of metastable M-buserite intermediates, which contain two layers of water (white spheres) in between the Mn-oxide layers. By drying at mild temperatures, one layer of water is removed and different M-birnessites can be isolated* [2]. *Image adapted from* [2].

Everything starts from an aqueous solution of two hydrated salts precursors that contain the two transition-metals needed for the oxide synthesis: Calcium-nitrate-tetrahydrate ($Ca(NO_3)_2 \cdot 4H_2O$) and Manganese-chloride-tetrahydrate ($MnCl_2 \cdot 4H2O$). The Ca/Mn molar ratio was maintained constant in most of the experiments and set equal to ½. Specifically, in case of each synthesis experiment, 2mol of calcium precursor and 4mol of manganese precursor were used. Into this solution, one added (under stirring) the appropriate amount of an IL (see Table 2.2). The oxidant had been dissolved (in case of all samples) to the pre-prepared solution, 2.5ml of NaOH (0.8M) under stirring awaiting that the reaction (Figure 2.1) reaches the equilibrium (≈30min). The total reaction volume was equal to 20ml.

Table 2.1 *Reagents and solvent amounts corresponding to the each concentration of the ionic liquid.*

Sample	Water (ml)	$Ca(NO_3)_2 \cdot 4H_2O$ (mg)	$MnCl_2 \cdot 4H2O$ (mg)	Ionic liquid (g)	NaOH 0.8M (ml)
None I.L.	17,5	472,3	791,64	0	2,5
Minimum I.L. conc.	17,3	472,3	791,64	0,2	2,5
Low I.L. conc.	15,5	472,3	791,64	2	2,5
Medium I.L. conc.	11,5	472,3	791,64	6	2,5
High I.L. conc.	5,5	472,3	791,64	12	2,5

During this last step, a change in the solution colours occurs. In fact, upon addition of the sodium hydroxide, the colour changes from transparent, at first to a light brown, and, at the end (after 30min), to a more dark one (see Figure 2.2). This change is due to the formation of a heterogeneous sediment mixture, probably composed of manganese/calcium oxides/hydroxides and calcium manganese oxide. When the stirring was interrupted, the sediments precipitated to the bottom.

Figure 2.2 *Colour evolution during the reaction.*

Subsequently, the sample was heated in a stainless steel autoclave with a PTFE core (≈23ml of free volume), at 180˚C (with a heating rate of 5°C/min), in order to allow

the formation of a large and ‘’orderly’’ structure as similar as possible to the natural CaMnOx present in the OEC complex.

The use of an autoclave instead of a normal flask, allows to keep a constant reaction volume by avoiding any losses of water.

Mixing, inside the autoclave, is carried out without any stirrer by means of a convective motion of the boiling water.

Figure 2.3 *Images of the autoclave used.*

After 8h of heating, the sample was collected in a tube and washed/centrifuged several times with water and ethanol. The recovered solids were dried at 100°C.

Lastly, the mixture was heated; this process is also called annealing or calcination, at high temperature (300°-500°; heating rate= 5°C/min), in such a way to lead to a more complete oxidation and to arrange the oxide structure.

All these steps were repeated upon use of the different ionic-liquids and under different conditions (see Paragraph 2.1.1).

2.1.1 Compounds synthesized

As explained in the first chapter, there are many kinds of ionic liquids, each and every one with its own features that lead to different interactions with a co-solvent (water) and precursors (Ca and Mn salts). This leads to different structures and porosity of the final product.

With the aim to find an efficient catalyst for the water splitting half-reaction, the project started from the use of a wide variety of ionic liquids after which the task was to select and concentrate on a smaller group of ILs synthesized by discarding the

samples with a less activity and keeping only the best. After this first selection, we had tried different concentrations of IL and different operative conditions under annealing (Table 2.2).

Table 2.2 *List of synthesized compounds.*

Ionic liquids	Concentration (g/ml)	Time of annealing	Temp. of annealing
/	/	1h/3h/5h	No/300°C/500°C/700°C
[Bmim]BF4	0,01/0,1	1h/3h/5h	No/300°C/500°C
[Bmim]PF6	0,01/0,1	1h/3h/5h	No/300°C/500°C
[Bmim]Cl	0,01/0,1/0,3/0,6	1h/3h/5h	No/300°C/500°C
[HMTA]Cl	0,01/0,1	1h/3h/5h	No/300°C/500°C
[Bmim]NTf2	0,01/0,1	1h/3h/5h	No/300°C/500°C
[HMTA]NTf2	0,01/0,1	1h/3h/5h	No/300°C/500°C

In nature, the OEC complex is composed of a main structure of manganese oxide with some vacancy, occupied by calcium atoms that modify and twist the oxide structure.

In order to understand the role of calcium in the catalytic process, it has been first synthesized with the same procedure; the only difference was that manganese oxide was compared in terms of its activity with that of thermally ("classically prepared") calcium manganese oxide.

2.1.2 Other synthesis methods

In literature as it already explained, there are several methods to synthesize CaMnOx and the most popular one is probably the one that we have illustrated. However, the so called ''precipitation method'' has many variations. For example, beyond the one described in the paragraph 2.1, a lot of articles make use of potassium permanganate ($KMnO_4$) as an additional precursor and, therefore, the catalysts prepared by comproportionation reactions of Mn^{2+} and MnO_4^-. This would lead (they say) to particles of α-Mn_2O_3 and $CaMn_2O_4 \cdot xH_2O$ with enhanced surface areas [47] and due to the very high affinity of MnO_6-layers for divalent cations. Thus, it would be possible to incorporate large amounts of alkali earth ions in the materials, even if 10–100 times higher concentrations of Na^+ or K^+ are present in the reaction mixture [2].

Therefore, it was tried also to experiment this new procedure following the one that is described in article [47]. Unfortunately, given "tight times" on this project and because

of the many variables at stake, it was not possible to deepen and optimize this technique to get successful results.

2.2 Analytical methods: activity measurements

Following the synthesis part, all produced materials were tested via activity measurements and then characterised by measuring the surface area, bulk/surface composition and structural analysis.

During the activity tests, three different strategies were followed.

The first one was to use the Clark Electrode for oxygen production measurements (common instrumentation for obtain curves of oxygen evolution in time). However, after some tests, this type of instrument proved to be inaccurate and influenced by many variables related to human, instrumental and environmental factors. This made it difficult to get reliable and repeatable results with acceptable errors.

For this reason, it was decided to adopt a different strategy which consisted of the use of gas chromatography. This choice proved to be exact, and it allowed for to get good results in terms of accuracy and sensitivity.

As third technique, CV/LCV was also used in order to verify the results already obtained by GC.

2.2.1 Clark Electrode

Clark electrode is an instrumentation invented by Leland Clark in 1956 with the aim to measure, in an amperometric way, the oxygen concentration. It remains one of the most commonly used devices for measuring the partial pressure of oxygen (sometimes referred to as ‘oxygen tension’) in the gas phase or, more commonly, dissolved solution.

The name ‘’ Clark electrode’’ is just one of the many titles often employed to describe this electrochemical sensor for oxygen. Other names include ‘’Clark Cell’’, ‘’Oxygen Electrode’’ and ‘’Oxygen Membrane Polarographic Detector’’ (O_2-MPD for short), because of the mode of action of the electrochemical device[48].

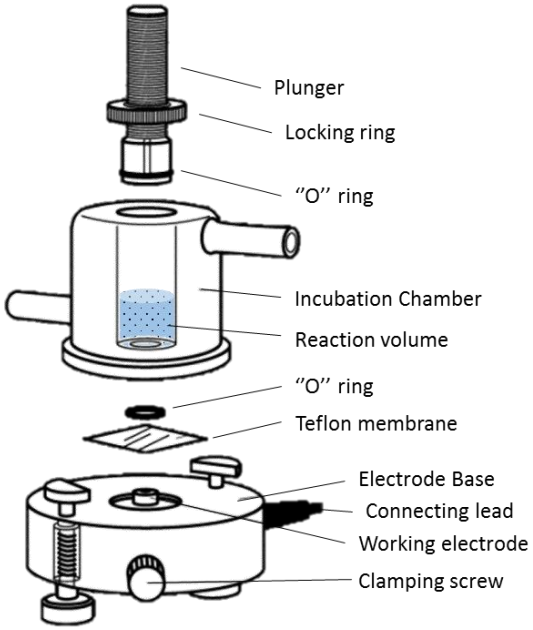

Figure 2.4 *Structure of the instrumentation. Image adapted from* [48].

The Clark cell utilised for measuring the catalytic activity of samples is made up of an electrode base where cathode and anode take place, a Teflon membrane, an incubation chamber to maintain the cell thermostated and a plunger in order to avoid the entrance of air from the environment (see Figure 2.4).

The electrode base comprises of two electrodes. The first one is a small (typically 2 mm in diameter) central platinum disc working electrode (this is the cathode and it is at this electrode that the O_2 diffusing through the membrane is reduced). Set in a well surrounding as anode there is a silver ring (Ag/AgCl) counter and reference electrode (about ten times larger in surface area than the platinum cathode). The conduction between the two electrodes is achieved using a 3M potassium chloride solution to saturate the paper tissue covering the two electrodes. On top of this, the key-element, a gas-permeable membrane, is installed: usually a 12.7 μm thick PTFE, sealed from the test sample in the incubation chamber by a silicone rubber ‘’O’’ ring [48].

The electrode base is connected to a controller that applies a voltage to the central platinum electrode that is sufficiently negative, with respect to the silver electrode, that all the oxygen diffusing through the gas-permeable membrane and reaching this electrode is reduced according to the reaction:

$$O_2 + 2H_2O + 4e^- \rightarrow 4OH^- \quad (2.1)$$

For every reduction cycle, there must be an oxidation and this occurs at the silver electrode as follows:

$$4Ag + 4Cl^- \rightarrow 4AgCl + 4e^- \quad (2.2)$$

Thus, the overall electrochemical process that occurs in on an oxygen electrode becomes:

$$4Ag + O_2 + 2H_2O + 4Cl^- \rightarrow 4AgCl + 4OH^- \quad (2.3)$$

The resultant current which flows between the two electrodes is proportional to the oxygen partial pressure in the test system, P_{O_2}. The controller converts this current directly into a voltage and it will display this in units of percentage of saturation. It is also measured continuously by using a data logger. The results of analysis will be in the form of a graph: mV vs. time(s) [48].

The polarising voltage at the platinum electrode is so negative that the current, i_d is related to the P_{O_2}, via the following expression:

$$i_d = \frac{4 \cdot F \cdot P_m \cdot A \cdot P_{O_2}}{b} \quad (2.4)$$

where F = Faraday's constant (9.64 × 104 C·mol−1), P_m = O_2 permeability of the PTFE membrane (typically 1.05 × 10^{-12} mol·atm^{-1}·s^{-1}), A = surface area of the platinum working electrode (typically 0.031 cm^2) and b = thickness of the PTFE membrane (typically 12.5 × 10^{-4} cm). Thus, in a test medium which is an air-saturated water, P_{O_2} = 0.2 atm, the oxygen electrode would give the approximate value for the i_d of 2 μA.

The oxygen electrode consumes oxygen from the test medium reaction (see equation 2.3). However, if the electrode is to function properly, it is important that the partial pressure of O_2 at the interface between the membrane and the test medium should be the same as that in the bulk of the medium. As a result, when the test medium is an aqueous solution, it must be continuously stirred; failure to do so will lead to a signal that drifts downward and general erratic behaviour. It can be shown that the percentage of the total amount of oxygen lost per minute (%D) from an aqueous solution of low ionic strength is given by the following expression:

$$\%D = \frac{12.5 \cdot i_d}{P_{O_2} \cdot V_{test}} \quad (2.5)$$

where V_{test} is equal to the volume of the test solution in dm^3 and i_d is the current flow through the electrode. For example, if we take i_d=2 μA for a sample where P_{O_2}= 0.2 atm (i.e. an air saturated solution), we can estimate that only if $V_{test} < 0.125$ cm^3 will the electrode consume > 1% of the total number of oxygen molecules present per minute. It follows from equation (2.5) that the measurements of P_{O_2} carried out on small isolated volumes of aqueous solution using the oxygen electrode should be avoided since it is likely to lead to a downwardly drifting signal as monitoring proceeds (due to oxygen consumption by the electrode). In such circumstances, it is better that the electrode is operated for short times rather than continuously [48].

Setup and calibration procedures

The procedure needed for set up and calibrate the instrumentation (Digital Model 10, Rank Brothers Ltd) is composed by the following step:

1. Plug the instrument into your mains supply, switch on and allow 5 minutes warm up. Ensure the electrode is not plugged in.

2. Adjust the Set Zero control until the display reads zero.

3. Adjust the polarising Volts control until a suitable polarising voltage is set (typically 0.6 V).

4. Using the teat pipette, wet both electrodes and fill the small well containing the silver electrode with the potassium chloride solution (3M).

5. Cut a 1.5 cm square piece of tissue paper with a 2 mm hole in its centre and float this on the potassium chloride in the well ensuring that the hole is central above the platinum electrode.

6. Touch the empty teat pipette against the tissue paper and use it to suck off the excess electrolyte so that the paper is wet (but not very wet) and clings to the surface of the electrode.

7. Cut a 1.5 cm square piece of PTFE membrane and place it so that it covers both electrodes, ensuring that the platinum electrode is underneath the centre membrane and that there are no air bubbles trapped under the membrane.

8. Gently push the silicone rubber 'O' ring over the platinum electrode so as to hold the PTFE membrane in place when the plastic base and the incubation chamber are clamped together.

9. Carefully clamp the electrode base and the incubation chamber together.

10. Connect the electrode to the controller, adjust the polarising voltage to 0.6 V and adjust the stirring speed to a suitable level. Connect the water jacket of the incubation chamber to a constant temperature water bath and allow the sample temperature to stabilise. The electrode is now ready for calibration.

11. Plug in an oxygen electrode that has been set up with water in the incubation chamber.

12. Sit the electrode on the stirring head and lock off with the white plastic retaining screw.

13. Circulate water through the electrode incubation chamber and allow the sample temperature (20°C) to stabilise.

14. Switch on the stirrer and adjust the stirring speed, typically around 6.

15. Bubble air through the water and allow the reading to stabilise.

16. The Sensitivity control can now be adjusted until the display reads 100.0 percentage saturation.

17. Purge all the oxygen from the sample by bubbling nitrogen through.

18. If the display does not read zero, this is due to residual current flow in the electrode, and can be trimmed out with the Set Zero control.

19. Adjusting the Set Zero will affect the calibration, so repeat steps 15, 16, 17 and 18 as necessary. The electrode is now calibrated and ready for use.

Sample test procedure

Conclude set-up and calibration part, the following point must be follow:

1. Prepare a cerium(IV) ammonium nitrate solution 2.4M and purge the oxygen dissolved by bubbling nitrogen through for at least 20min.

2. Prepare a catalyst suspension (1mg) in 0.9ml of water and dropped it inside the cell.

3. Close the top of cell with the plunger.

4. Purge all the oxygen from the sample by bubbling nitrogen through.

5. Inject 0.1ml of cerium(IV) solution in the cell by using an air tight syringe.

Figure 2.5 *Clark Electrode used during a measurement.*

2.2.2 Gas Chromatography

Chromatography is the process of separating a mixture into individual components. Through the separation process, each component in the sample can be identified (qualitatively, not always) and measured (quantitatively). There are several kinds of chromatographic techniques with corresponding instruments. Gas chromatography (GC) is one of those techniques. GC is used for compounds that are thermally stable and volatile (or can be made volatile). Because of its simplicity, sensitivity and effectiveness in separating components, GC is one of the most important analytical tools in chemistry. The basic operating principle of a GC involves evaporation of the sample in a heated inlet port (injector), separation of the components of the mixture in a specially prepared column and detection of each component by a detector. At the end of the process, the amplified detector signals are often recorded and evaluated using

an integrator or a personal computer (PC) with appropriate software to calculate the results. The sample is introduced into a stream of inert gas, the carrier gas, and transported through the column by the flow of this carrier gas (see illustration below, Figure 2.6). The column can be a packed column or a capillary column, depending on the properties of the sample. As the gas flow passes through the column, the components of the sample move at velocities that are influenced by the degree of interaction of each component with the stationary phase in the column. Consequently, the different components separate. Since the processes are temperature-dependent, the column is usually contained in a thermostatically controlled oven. As the components elute from the column, they can be quantified by a suitable detector and/or be collected for further analysis [49].

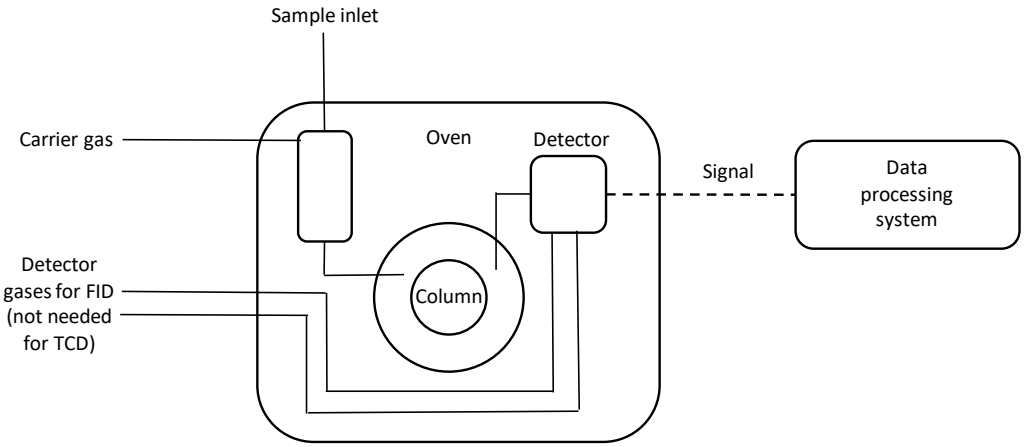

Figure 2.6 *General scheme of a Gas-chromatograph.*

There are a lot of different kinds of detectors and the choice of it depends from the type of component(s) to be detected and measured. The most common detectors are: Flame ionisation detectors (FIDs), thermal conductivity detectors (TCDs), electron capture detectors (ECDs), alkali flame ionisation detectors also called nitrogen/phosphorous detectors (NPDs), flame photometric detectors (FPDs) and photo ionisation detectors (PIDs).

Anyway, for the transportation of the sample through the column, a carrier gas is needed. This gas enters with a constant flowrate (through the inlet, column and detector) where if it is fluxed alone it represents the blank signal. However, when the sample is injected, the carrier gas does not have to react with it and neither with the stationary phase of the column, so for these reasons it must be an inert gas. Helium,

nitrogen, argon and hydrogen are commonly used as carrier gases. The choice depends on the type of detector, column, application and safety requirements (for example hydrogen is explosive and so hazardous). However, the choice can be influenced also by its separation efficiency and speed [49].

Columns can be divide in 2 categories: Open Tubular Columns and Packed Columns. The first is also called capillary column and it consists in a wall-coated open tubular column or in a porous layer open tubular while the second type is a support-coated open tubular column. The basic principle, on which separation is carried out, is mainly given by adsorption phenomena that in other words consists in the formation of a series of secondary bonds (dipole-dipole interaction, hydrogen bond, Van der Waals etc…) between the active sites present on the solid stationary phase and the different molecules of the sample mixture.

Specifications

Even if the project requires to quantify the oxygen as much as hydrogen production, by measuring only the oxygen, the hydrogen production can be considered as the stoichiometric product. Now that in order to reach a good separation of oxygen from an air mixture, helium was used as the carrier gas. Indeed, Helium, gives the best overall performance and peak resolutions for many applications, making it an optimum choice of carrier gas as in this case.

Regarding the detector, since the aim was to identify the relative amount of oxygen, and helium was employed as the carrier gas, it is obvious that the only feasible detector that could be used is the TCD one (FID cannot be used since it requires a hydrogen flame).

TCD is one of most common detectors for a GC and it is based on an electrically heated filament located in a thermostatic cell that contains a calibrated electrical resistance. When no sample is introduced inside a GC, only the carrier gas flows in the cell and this leads to a stable heat flow passing through a resistance. Once a sample is injected, after column separation, it enters in the detector body and thanks to different thermal conductivity of it, a change of the resistance occurs. This variation can be measured in mV (by mean of the Ohm law) usually with a Wheatstone bridge.

The GC used was an Agilent model 7820A (Figure 2.7), with a molecular-sieve-coated PLOT capillary column (J&W CP-Molesieve 5Å, see Table 2.3 for specifications) and manual injection.

Table 2.3 *Configuration choices for Agilent J&W CP-Molsieve 5Å* [50].

Capillary	
ID (mm)	0.25 – 0.32 mm
Length (m)	10 – 50 m
Film (µm)	10.0 – 30.0 µm
Temperature Limits (°C)	-200 – 350/350 °C

Regarding software configurations, we investigated many different operating conditions. The best one is reported below:

Inlet

- Temperature= 140°C
- Pressure= 4.8098 psi
- Split ratio= 10:1; 60 ml/min

Column & Oven

- Flow= 6 ml/min
- Hold time= 3.5 min
- Temperature= 110°C

Detector

- Temperature= 140°C
- Make-up flow= 2 ml/min

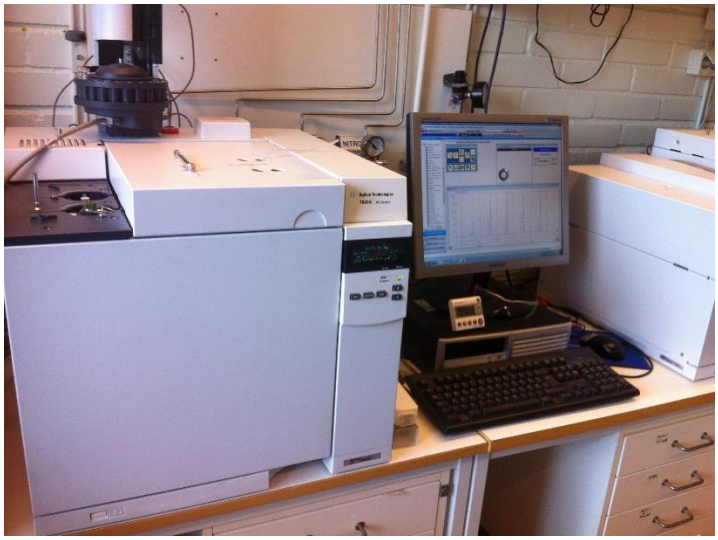

Figure 2.7 *GC-TCD system.*

Test procedure

The Overall procedure for GC Oxygen measuring can be summarized as the following steps:

1. Prepare a flask of distillate water saturated of Oxygen. Air must bubble for at least 20min.
2. A mass of 2 mg of catalyst and 0.2632 g of cerium-ammonium-nitrate was inserted (in order to obtain a reaction solution 2.4M).
3. Insert in a vial catalyst and cerium-ammonium-nitrate weighted in the previous step.
4. Insert into the same vial a magnetic stirrer.
5. Add 2 ml of oxygen saturated water and close the vial as soon as possible with a specific air-tight cap.
6. Immediately, sonicate the sample for 20s. This can be approximatively considered as the time-zero (when the reaction is initiated).
7. Insert the vial in a thermostatic bath at 40°C (Figure 2.8).
8. After 10min, purge at least three times a gas tight syringe with helium, using the GC outlet.
9. Collect with a syringe 100µl from the head-space of a vial.
10. Analyze the sample in the GC.
11. Repeat steps 8, 9, 10 for every ten minutes (for the first hour and then after every hour until the 3rd).

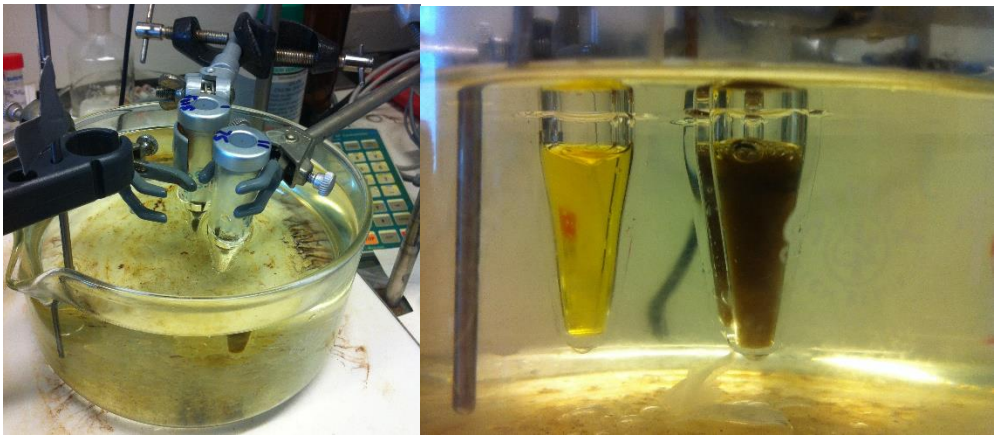

Figure 2.8 *Reactor set-up.*

2.2.3 Cyclic Voltammetry/Linear and linear sweep voltammetry

An alternative to Clark electrode and GC is offered by CV/LSV tests. It's part of electrochemical analysis and its principle is based in the measure of electrons flow that is achieved during an electrolysis process. In particular, for quantify the amount of current produced when the water oxidation take place, a fixed potential range is applied to the cell with a fixed rate. Furthermore, in a CV test, differently to LSV, when potential reach the final value it returns to the initial value. In this way also the opposite reaction is tested.

The setup used in our study was composed by a small cylindrical cell and a reference silver-chloride electrode, counter platinum electrode and a working carbon electrode where on the surface a layer of the catalyst was deposited (read forward about the preparation method of this). A solution 0.1M of NaOH acted as an electrolyte.

Carbon Electrode preparation method

Deposition began with a preparation of a matrix solution. 5 mg of the catalyst, 400 µl of isopropanol, 100 µl of water and 2.5 µl of Nafion were blended together, and sonicated for 30min. After that, 5 µl of this solution was added dropwise to the small back area of the electrode. Finally, after drying, the electrode was ready to be used (see Figure 2.9).

Figure 2.9 *CV/LSV set-up.*

2.3 Analytical instrumentation: catalyst characterization

2.3.1 Scanning Electron Microscope

One of the most widely used analytical tools during characterization phase, Scanning Electron Microscope (SEM) allows to capture pictures by scanning it with a beam of electrons. This instrumentation is able to show extremely detailed images that provide to characterize the texture and the crystalline/amorphous morphology of the sample and other stuff.

Operating principle

When accelerated electrons hit the solid surface of a sample, their kinetic energy is dissipated as a variety of way as: generation of secondary electrons (that produce SEM images), backscattered electrons (BSE), diffracted backscattered electrons (EBSD that are used to determine crystal structures and orientations of minerals), photons (characteristic X-rays that are used for elemental analysis and continuum X-rays), visible light, and heat. Backscattered electrons and secondary electrons are commonly used to acquire pictures of samples [51].

Sample preparation

Powder materials are hard to mount and need special handling for sample mounting. Otherwise they may get loose and fly off the holder in the vacuum and under the beam [52].

The amount of our samples was really low ($\approx 10^{-3}$g); in this case the best strategy is to disperse powder in a volatile solvent like acetone or an alcohol and then add the mixture dropwise onto a clean substrate.

Since calcium-manganese oxides are not very conductive, the charge effect may cause an image with distortion and drift. To completely eliminate the charge effect, some samples were coated with a layer of gold.

2.3.2 Inductively Coupled Plasma Optical Emission Spectrometry

In general, ICP is an analytic technique based on the use of the mass spectrometry combined inductively with a coupled plasma (this is the reason of acronym ICP).

It's a technique really sensitive (close to the order of magnitude of ppb) and it's able to determine the composition and the amount of specific elements that compose a given sample.

The instrument exploits a plasma torch in order to induce an ionization of the sample, and then a mass spectrometry for the separation and revelation of the produced ion.

In particular, once the sample is injected in the ICP-OES (usually by means of a peristaltic pump and then a nebulizer) the produced aerosol, by passing through the argon plasma (held by an alternate magnetic field), it split itself in its elemental component (an ensemble of ions). Successively, thanks to the thermic energy absorbed by elements from plasma, it's electrons reach first an excited state for then drop back to the base energy level. In this transition phase, photons are produced and released. Composition (with the relative amounts) is therefore detected by means of the mass spectroscopy known that each element is characterised has a specific and unique emission spectrum.

Sample Preparation

To be analysed with ICP-OES, a sample has to be dissolved. This is usually conducted with the help of nitric acid. After that, this solution was diluted in order to avoid any corrosion of the instrumentation components.

In this way, our samples were dissolved in the so called ‘’matrix solution’’ with acid. However, with HNO_3 67% w/w, the calcium-manganese oxides still remained at the tube bottom. For this reason, while being recommended the use of nitric acid for this type of analysis (because it doesn’t create any interference), we had to use hydrochloric acid 37% w/w, which led to total dissolution of the catalysts. Thus, for each sample we prepared a ‘’Matrix’’ composed of 1 mg of catalyst and 2 ml of HCl; then, 20µl of matrix solution was diluted in 10 ml of distilled water (dilution factor= 1:500).

Before any analysis, the instrument was calibrated utilizing the calibration curve obtained from the means of three points obtained from three samples of Ca at assigned concentrations (0.01ppm; 0.1ppm; 1ppm). In case of manganese, a similar procedure was applied.

Figure 2.10 *ICP-OES.*

2.3.3 Volumetric Gas Adsorption: Nitrogen Adsorption

Surface area and porosity are probably two of the most important physical properties for a catalyst and these have a strong impact on its activity. Indeed, during catalysis process, only its surface take part to the reaction while the bulk, not being in contact with reagents, works like an inert material. This means that more surface area is equal to say more activity per grams of catalyst.

The measurement is performed by means of the technique known by the name of "Volumetric Gas Adsorption". An Inert Gas (Nitrogen in our case) are introduced using a discontinuous, point-by-point procedure where at each stage the system is allowed sufficient time to attain equilibrium, which of course corresponds to a series of single points on the adsorption isotherm [53]. After reaching the maximum value of pressure p/p^0, the process is repeated in a reverse way until return back to the initial situation [53].

The isotherm curves are usually reported in absorbed volume against its relative pressure. The shape depends on the texture of the porous solid and so from its behaviour in absorbing an inert gas (as in this case nitrogen). By the way, it's also important to underline how this behaviour can change between absorption and desorption phases. In that case, we will observe a hysteresis in the resulted isotherm curve. This is due to pore shape and it happens because of two main reasons:

- **Tensile strength effect (TSE)** caused by the ink bottle shape of pores. Here, nitrogen condensation takes place during the adsorption phase, while in the desorption phase of the nitrogen you will need a greater pressure gap to exit from the pore body seen that the latter is filled with liquefied gas. In this way the two curves of absorption/desorption will show two different trends.
- **Capillary condensation** (which a typical phenomenon that testify the presence of mesoporousity). The molecules are adsorbed on a surface because of the force field exerted on them by the pore walls. In the mesoporous materials, molecules get adsorbed layer by layer (filling firstly the higher energy sites near pore wall and then low energy sites away from wall). After that molecules accumulated on two opposing walls get close enough to each other, they collapse into a thermodynamically lower energy state. Follows that, if you reduce pressure during desorption the molecules at low energy will not tent to leave their place, so you need higher gradient of chemical potential (or equivalently pressure drop) to pull the adsorbed molecules out of their sites. The result is that the same molecules desorb at lower pressure. This gap, between equilibrium adsorption and desorption pressures, cause the hysteresis.

According to IUPAC classification, there are four types of hysteresis that can be easily distinguished during a catalysts characterization [53–57]:

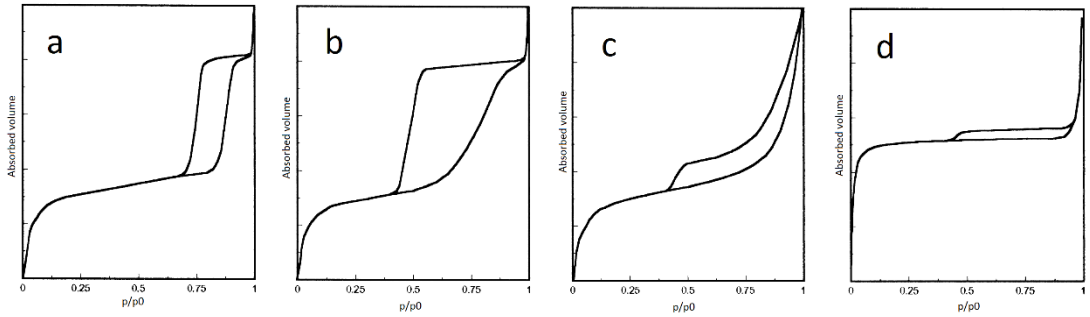

Figure 2.11 *Examples of the four hysteresis types classified by IUPAC. Image adapted from* [59].

‘’a’’ and ‘’b’’ usually are the characteristic curves of nearly cylindrical channels particles, or solid made of aggregates/agglomerates of spheroidal particles while instead, ‘’c’’ and ‘’d’’ are usually found in aggregates/agglomerates of particles forming lit shaped pores (plates or edged particles like cubes) [59].

Sample preparation

Instrumentation used was Micrometrics Tristar model 3000. The following steps were related to this model. However, there are no significant procedure changes between the various models and brands.

Since all the testing occurred inside a little flask and, since the analysis results are expressed in units of surface area per gram of sample, the true sample mass must be known. During all weighing steps it was important not to touch the sample with bare hands since this could have an adverse influence on the accuracy of the results.

First at all, the sample tube was weighted empty. As the next step, the sample was introduced into it. If some sample sticks to the inside of the sample tube above the red line (see Figure 2.12), it was removed by using a pipe cleaner. Weighing was repeated.

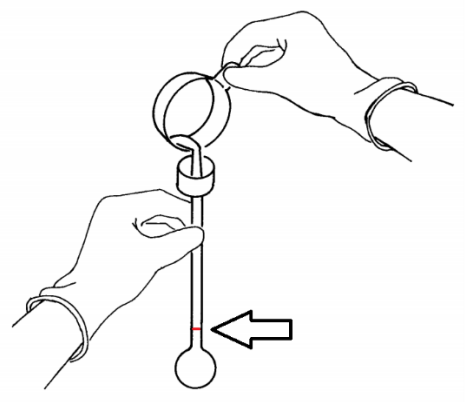

Figure 2.12 *Placing a sample in a sample tube. Image adapted from* [60].

After that, the sample was weighed, a degassing unit was used in order to remove any contaminants which may have been adsorbed to the surface or pores of the sample. The degassing conditions were: 120°C for 5h with a heating rate of 5°C/min, at an ambient temperature as well as under nitrogen atmosphere. Finally, when degassing was complete, the tube set containing the sample was weighed and recorded.

Once that these steps were completed, the samples tube was prepared and could be installed in the three ports available inside the instrumentation. Before start the analysis, the software required all weight relevant weight data (empty, before degas and after degas) that will use for the elaboration of the results.

2.3.4 X-ray Photoelectron Spectroscopy

Since the active part of a catalyst is only its surface, it is useful to understand its chemical composition and then compare it with the one of a OEC complex. Furthermore, in the water oxidation reaction, the main attention is attracted by the oxidation state of manganese. It is seen that the most active catalyst was obtained when the oxidation state of manganese was present as a mix of +3/+4. For this reason, we wanted to investigate this feature by running XPS analysis.

This kind of instrumentation exploits the principle that by shooting an atom or a molecule with an X-ray photon, an electron can be ejected. This electron, by absorbing the energy of the X-ray photon, gain kinetic energy in an amount in which depends from both the photon energy (express by hν) and the binding energy of the electron [61].

In this way kinetic energy of the electron ejected, if measured, can give important information on binding energy typical of each element/compound and orbital from which the electron is ejected, such to allow to obtain the composition, rather than the electronic configuration of elements that compose the sample.

2.3.5 Raman spectroscopy

Among all characterization analysis, we chose also this one. Raman-diffusion-spectroscopy it's a sort of ''revisitation'' of the more standardized IR-absorption-spectroscopy.

Both are vibrational spectroscopies and so in both cases the results depend from the behaviour of sample's molecules struck by a beam of photons. Furthermore, both instrumentations are physically constituted by a light source, monochromator, spectrometer and detector.

A main difference between these two techniques comes from their names: IR uses adsorption phenomena while Raman exploits the diffusion phenomena (scattering). Indeed, when a monochromatic radiation is incident on the surface of an object, the radiation can be:

- Absorbed if it has an energy equal to a possible transition to a higher energy level.
- Reflected if it does not interact with matter.
- Widespread, it is interacting without causing energy transitions.

In Raman-scattering-spectroscopy after the sample is struck by an electromagnetic radiation of known intensity and frequency, the scattered radiation is measured using a detector placed at 90º or 180º with respect to the optical path along the sample (in IR spectroscopy is placed along the optical path directly after the sample). The radiation can be spread in three ways: Stokes, anti-Stokes and Rayleigh (elastic scattering). The Stokes radiation has less energy than the original incident radiation, as a part of this energy is used to promote a transition to a higher level. The anti-Stokes radiation instead receives a contribution of energy from the excited state when it passes at a lower level, for which is characterized by increased energy. The Rayleigh scattering

of radiation comes from an elastic scattering and has the same energy of the incident radiation.

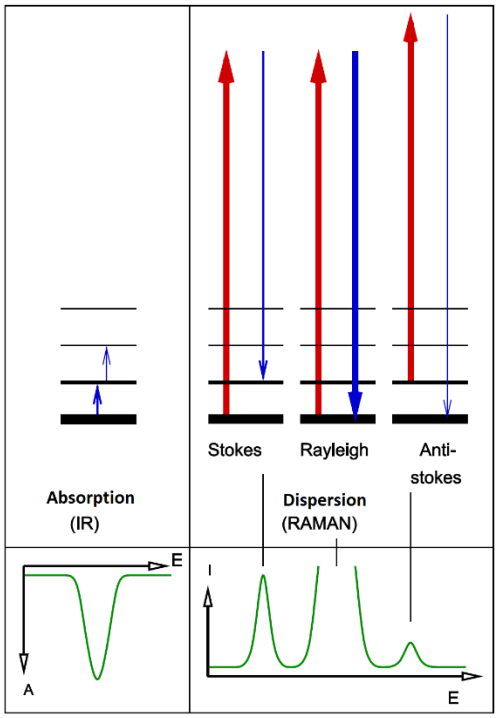

Figure 2.13 *Diagram of different energy levels involved in the transitions studied by Raman spectroscopy. Notice how the Stokes radiation possesses less energy than the incident radiation, while the anti-Stokes has a higher energy content. Image adapted from* [62].

Note that in order to obtain a Raman signal the sample in analysis have to be anisotropically polarizable in the case of rotational transition, i.e. the vibration must entail a variation of the polarizability in the case of molecular vibration. The so-called "exclusionary rule" states that if a molecule has a centre of symmetry no vibrational mode can be simultaneously Raman-active and active-infrared.

Figure 2.14 *Raman spectroscopy device.*

These analysis has been conducted in a Renishaw Invia Raman Confocal Microscope (Figure 2.14) within the range 200-1500 cm^{-1} using 514 nm laser (Modu-Laser, Stellar-REN model) for 10s/scan at 5% of power with a 2400l/mm grating. Measurements were performed on BaF_2 glass. Before scanning every samples, the background spectrum of BaF_2 without the sample was taken and subtracted.

Chapter 3

Results and discussion

This chapter resumes and discusses all the results obtained during this project. So herein, all the results obtained from activity and characterization tests performed with techniques and methodologies illustrated in the Chapter 2 are summarized.

As already explained, the activity of our compounds were tested mainly via two different techniques: The Clark electrode and Gas-chromatography. The reason is mostly due to the fact that in order to affirm that a catalyst has a specific activity, it's of fundamental importance to guarantee that this result can be obtained from everyone in the world, hopefully also with a different way of measurement (repeatability of the experiment).

In particular, these methods were chosen since they are the most common ones in the literature for this kind of investigations and this renders it easier to compare the results.

The characterization analysis was performed only on the samples considered as the most promising ones or for some reason of particular interest.

3.1 The variables selected

Upon each problem that we want to solve or question what do we want to answer, a selection of variables has to be done.

The study involved a lot of different variables that can be divided in two main groups: the synthesis and activity variables.

During this work we have selected only the variables of each group that have a fundamental role in the final catalyst performance:

Synthesis variables

- Total reaction volume;
- Concentration of precursors;

- Anion of precursor;
- Ca/Mn molar ratio;
- Type of ionic liquid (anion and cation effect);
- Annealing effect;
- Annealing temperature;
- Annealing time;

Activity test variables

- Reactor temperature (GC test);
- Lifetime of the catalyst (GC test);
- Catalyst deposition procedure (CV/LSV tests);

3.2 Activity tests: The Clark Electrode

3.2.1 Elaboration of data

As previously mentioned, the output signal of a Clark Cell consists in the current that flows between Pt and Ag/Cl electrodes. The controller converts the current from the electrode to a voltage and the results data is given in a mV vs time graph. Thus if S is the voltage from the controller, it is proportional to the partial pressure of O_2 in the medium under test:

$$S - S_0 = K \cdot P_{O_2} \tag{3.1}$$

Where K is the proportionality constant that depends from the setting of sensitivity control on the instrument and S_0 is the background signal when P_{O_2} = 0 atm. Knowing that the partial pressure in 100% air-satured water (as specified in the operating manual[48]) is the follow:

P_{O_2} = 0.2095atm = 159 mmHg

and the initial mV values of the graphs correspond to the one of air-satured water, the proportionality constant K can be found for each measurements thanks to the equation (3.1) inverse:

$$K = \frac{S - S_0}{P_{O_2}} \tag{3.2}$$

In this way we have the possibility to correlate output signal (mV) to partial pressure of O_2 through the inverse of (3.1) equation.

However, activity test results, on this kind of catalyst, usually show graph based on O_2 mole production and not on his partial pressure variation. In order to achieve this conversion is reasonable assume that oxygen is slightly soluble in water and so Henry's law can be exploited:

$$C_{O_2} = H \cdot P_{O_2} \tag{3.3}$$

Where C_{O_2} is the concentration of Oxygen in liquid and H is the Henry's constant typical of each gas (at 298.15 K for Oxygen $H = 1.3 \cdot 10^{-3}$ mol/atm·L).

Our tests occur in a thermostated cell at 20°C (293.15 K), so since Henry's constant is dependent on the temperature, van't Hoff equation has been used:

$$H(T) = H^0 \cdot exp\left[\frac{-\Delta_{sol}H}{R}\left(\frac{1}{T} - \frac{1}{T^0}\right)\right] \tag{3.4}$$

where R is the universal gas constant, T^0 the reference temperature (298.15 K) and $-\Delta_{sol}H$ is the enthalpy of dissolution (for O_2, $\frac{-\Delta_{sol}H}{R} = 1700\ K$). Note that van't Hoff equation in this form is only valid for a limited temperature range in which $-\Delta_{sol}H$ does not change much with temperature.

3.2.2 Analysis results and discussion

As the first approach, the test battery was composed of compounds synthesized from different ionic liquids, at different concentrations, keeping constant the other variables (see Table 3.1). Moreover, all samples were tested before annealing phase and then these results were compared with those after annealing. Note that every test was repeated at least for three times. The results shown are the average of all repetitions.

Table 3.1 *Group of compounds initially tested (variables: concentration and type of ionic liquid).*

Sample	Water (ml)	$Ca(NO_3)_2 \cdot 4H_2O$ (mg)	$MnCl_2 \cdot 4H2O$ (mg)	Ionic liquid (g)	Type of ionic liquid	NaOH 0,8M (ml)
0	17,5	472,3	791,64	0	/	2,5
0X	17,5	/	791,64	0	/	2,5
KMnO4	17,5	472,3	791,64	0	/	2,5
A1	17,3	472,3	791,64	0,2	[Bmim]BF4	2,5
A2	15,5	472,3	791,64	2	[Bmim]BF4	2,5
B1	17,3	472,3	791,64	0,2	[Bmim]PF6	2,5
B2	15,5	472,3	791,64	2	[Bmim]PF6	2,5
C1	17,3	472,3	791,64	0,2	[Bmim]Cl	2,5
C2	15,5	472,3	791,64	2	[Bmim]Cl	2,5
D1	17,3	472,3	791,64	0,2	[N-allyl-HMTA]Cl	2,5
D2	15,5	472,3	791,64	2	[N-allyl-HMTA]Cl	2,5

Regarding the type of ionic liquids used, the choice was made from two cations and three anions for then interchange and pair them in their different combinations (Table 3.1). Thereby, the different observations and roles that cations and anions play in the iono-thermal synthesis were analysed.

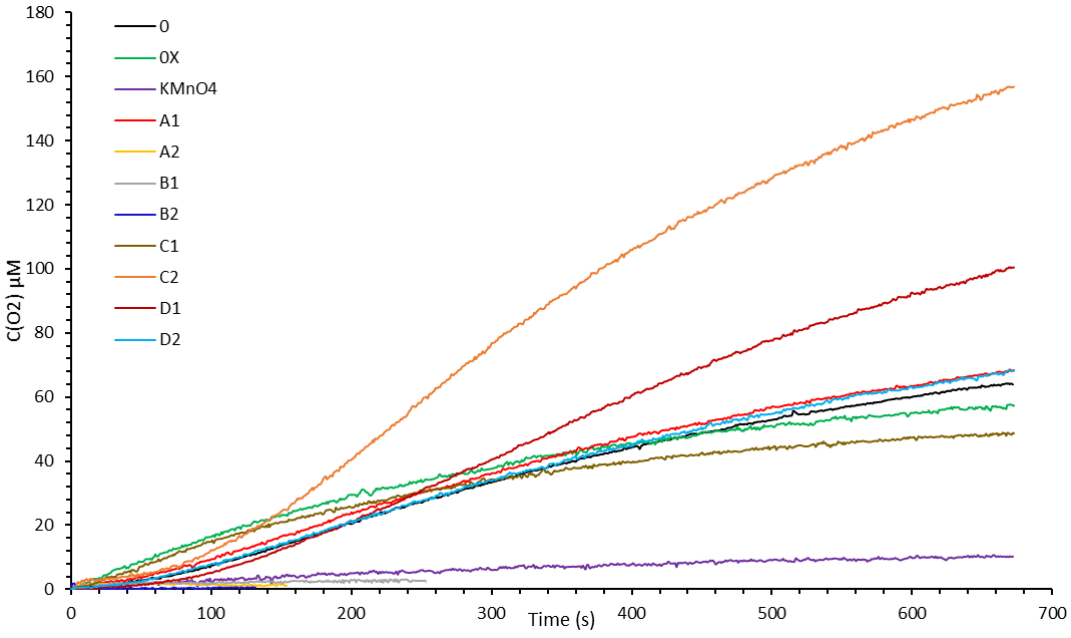

Figure 3.1 *Overview of catalysts activities measured with Clark Electrode (1ml of water, 2.4M of Ce^{4+}, 1mg of catalyst).*

Figure 3.1 gives an overview of all test runs by means of the Clark Electrode. The legend refers to Table 3.1. The catalyst synthesized with 1-butyl-3-methylimidazolium chloride ([Bmim] [Cl], sample C2) seems as the best, in fact its activity is more or less three times higher than the average of other samples.

Nevertheless, only the sample with higher concentration showed an improved activity in respect to the standard synthesized with the hydrothermal method. This means that

the low concentration of ionic liquid (as 10 mg/ml, sample C1) had no influence in terms of the oxide forming and, the interactions between reagent and solvent mixtures did not provide any improvement as compared to pure water

A second promising compound, from the point of view of its activity, was the sample synthesized with the help of [N-allyl-HMTA] [Cl] (sample D1). Indeed, after 10 min the oxygen production monitored was almost twice in respect to the standard sample 0. However, in this case, it is interesting to note how the relation between the concentration and activity was reversed if compared to the previous samples (C1, C2) since the sample D1 (IL conc.= 100 mg/ml) gave rise to a greater production of oxygen than D2 (IL conc. = 10 mg/ml).

$[N\text{-allyl-HMTA}]^+$ cation is really thermal sensitive, in particular in case of the HMTA complex (Hexamethylenetetramine, $C_6H_{12}N_4$), while the [N-allyl-HMTA] [Cl] decomposition occurred at 200°C.

The operative autoclave temperature was set to 180°C so there shouldn't be any problem: Nevertheless, since the reaction solvent was composed of a mixture with water, the interaction between the [N-allyl-HMTA] [Cl] and polar water molecules led to a premature decomposition of the ionic liquid. As a proof of that is that every attempt with this kind of an IL resulted in a formation of a heterogeneous powder containing small black residues of an unknown origin while the liquid part remaining after heating had a bad smell (see Figure 3.2).

Figure 3.2 *Unknown contamination in the CaMnOx synthesized with [N-allyl-HMTA] Cl.*

The loss of activity measured with a higher concentration and, therefore, the decrease of active sites on the catalyst mass could be justified by this contamination originating from the decomposition of the solvent.

The CaMnOx synthesized starting from potassium permanganate (curve KMnO4) did not give good results and, indeed, the production of O_2 was inferior to that of a standard sample. This suggests a problem of contamination as happened in the previous case with [N-allyl-HMTA] [Cl]. The procedure followed for that synthesis required dissolution of $KMnO_4$ in a really large amount of KOH (150 mmol of potassium hydroxide every 4 mmol of manganese). Thus, a lot of potassium remained and contaminated the final product. On the other side, a large amount of KOH is needed to change the oxidation state of Mn. In fact, potassium permanganate in a water solution is present as ions K^+ and MnO_4^- and, therefore, in order to transform permanganate VII (MnO_4^-) to permanganate VI (MnO_4^{2-}), a strong alkaline environment is needed. As a confirmation of that a change of solution's colour occurs from purple to green. In any case, no justification regarding this step has been provided in the reference where this procedure was explained ([47]). As mentioned in paragraph 2.1.2, due to the time constraints, it was not possible to delve into the details of this method much less to optimize it.

Among all, a lower activity was observed for the samples A2 and B2 that were synthesized using [Bmim] [BF_4] and [Bmim] [PF_6], at moderate concentrations. It is important to underline that upon using ionic liquids containing fluorinated anions (as [Bmim] [BF_4] and [Bmim] [PF_6]) produced powder of white colour instead of light-brown as expected for a CaMnOx sample. The change in colour takes place during the heating phase. In fact, before the autoclave step and after NaOH addition, the sample assumes the usual shade of brown. The anomaly could be caused by undefined ionic-liquid/reagents interactions at high temperatures (180°C), since ionic liquids with fluorinated anions, as PF6 and BF4, are not soluble in water and, therefore, remain in suspension contrary to what happens to those having the chloride anion, very soluble and very hygroscopic. The white colour suggests the formation of calcium oxide or a mixture of manganese and calcium carbonates - usually all transition metal oxides are brown or similar.

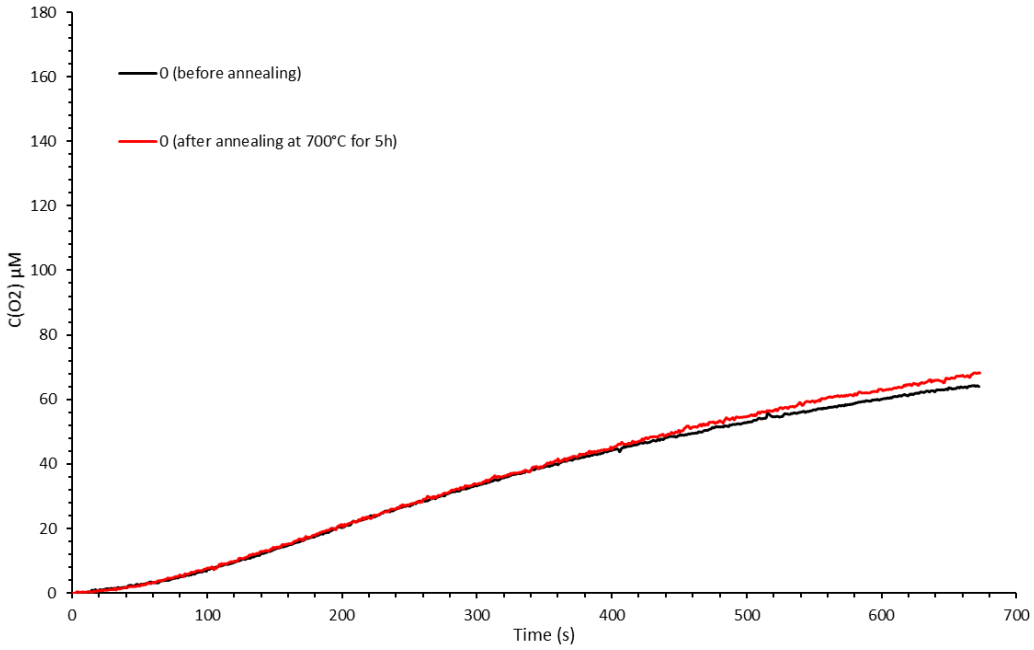

Figure 3.3 *A comparison between the standard sample before annealing and after annealing (at 700° for 5h).*

Figure 3.3 depicts the activity of the sample (standard sample 0) before and after heating treatment. The tests showed that the catalyst activity increased after annealing, even if the difference between the two curves is not really clear and could be justified by experimental errors. In fact, the real reason is the bad choice of annealing parameters as will be demonstrated in the next paragraph.

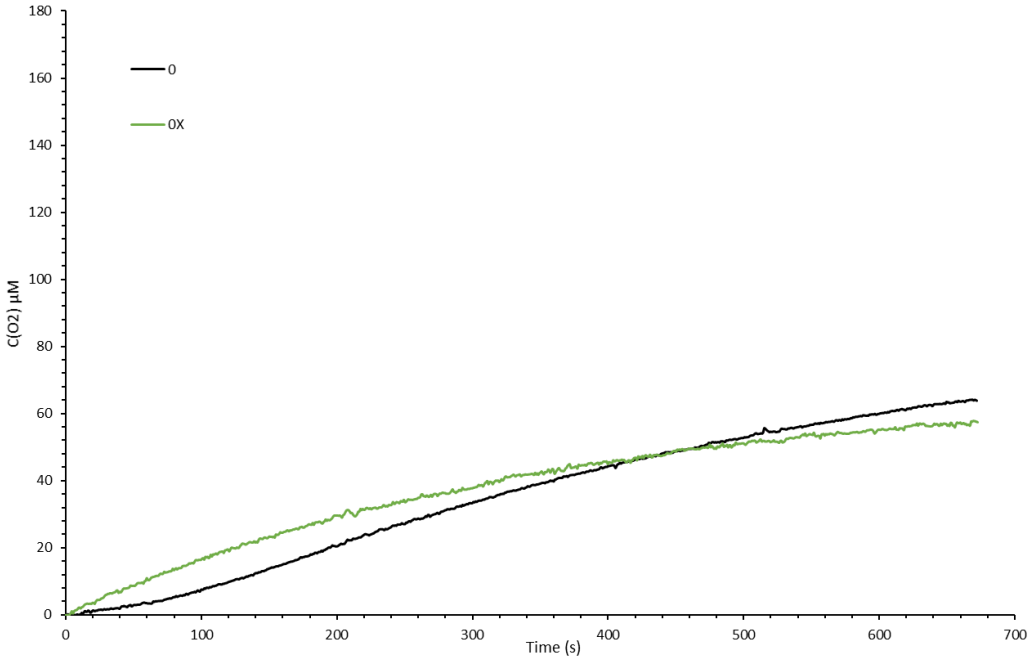

Figure 3.4 *The activity comparison between MnOx and CaMnOx.*

As already explained in the first chapter, it is known from the literature that calcium has a fundamental role during the water oxidation catalysis in the OEC complex. In order to verify the veracity of this statement, the activities of two samples were compared, both synthesized by means of hydrothermal method. One of them was made of CaMnOx while the other one did not contain Ca (only MnOx). Figure 3.4 highlights the positive influence that the presence of calcium has on the structure of the catalyst. Even in this case, the increase, although present, is not so too dramatic. Later, during the characterization phase we will try to justify this fact.

3.2.3 Issues when using the Clark Electrode

It is important to underline that even after an attempt of the instrumentation optimization, the Clark electrode outcome was inaccurate for a whole series list of reasons:

- in many cases, due to the motion of the bubbles, during the step of purging with nitrogen, the catalyst remained partially stuck on the chamber's walls and, in part, it went back through the plunger. Therefore, it no longer remained in contact with the reaction volume;
- the preparation and calibration procedure of the electrode is involved with many stages and, thus, many variables can easily affect in various ways the results of each analysis;
- the PTFE membrane, being a very thin, can be damaged compromising the results. We tried to reduce this risk by replacing the membrane at each measurement;
- the concentration of the electrolyte between the two electrodes (Pt-Ag/Cl) varies over time as the solvent is in continuous evaporation;
- mixing within the cell is not sufficient, and a part of the catalyst rather remaining in suspension, is deposited to the bottom causing it to be less efficient in the catalytic action and cannot operate at full capacity;
- the amount of catalyst used in each test (1mg) is too low and this leads, first, to errors upon scaling and, second, to not representative result taking into account that the samples in analysis were highly heterogeneous (as will be shown during the characterization). A greater quantity, therefore, would lead to more reliable results because of the average activity of a higher amount of

material. Unfortunately, this last solution was not applicable, since quantities above 1 mg would lead to a saturation of the instrument and to the consequent escape of oxygen from reaction volume to the head-space which is not monitored by the detector. In fact, has no influence on the current flowing between the two electrodes (narrowness of the instrument).

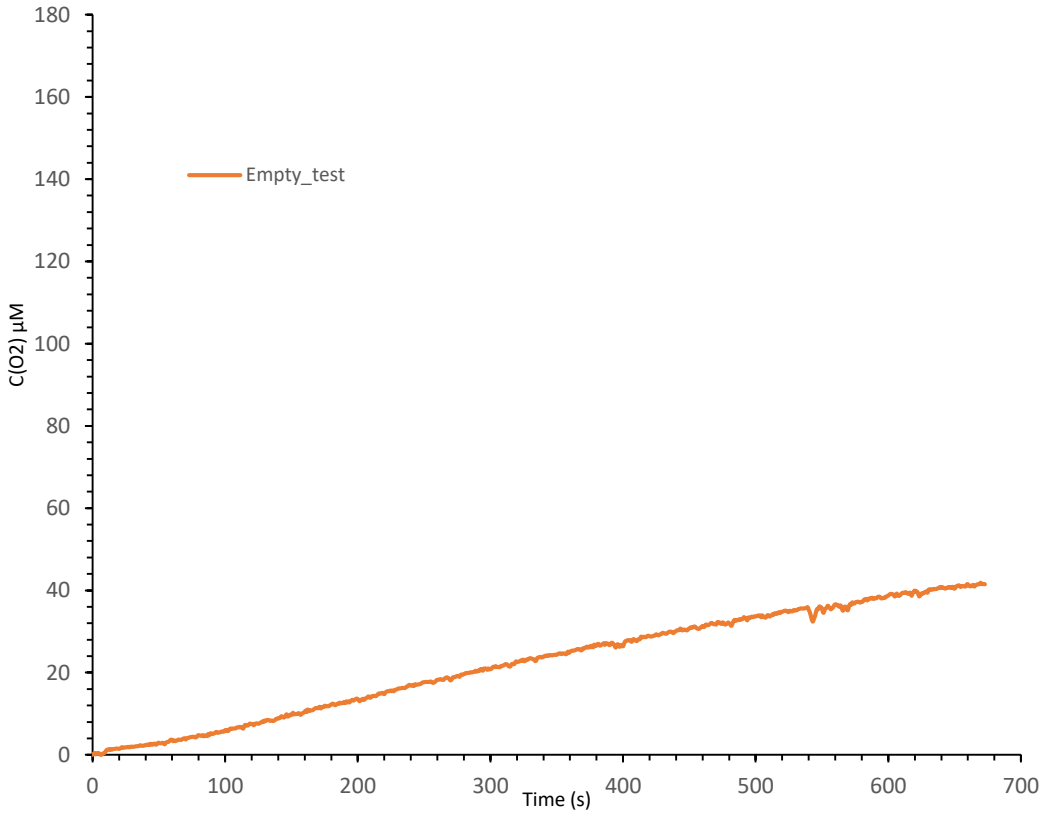

Figure 3.5 *Unexpected results with the Clark Electrode.*

"Empty tests" were often performed to verify the reliability of the instrumentation. In Figure 3.5 we note, for example, that the residues from previous analysis remained stuck to the wall surface or to the base of the chamber and could affect the results in a not negligible way.

3.3 Activity tests: Gas-chromatography

From the results obtained with the Clark Electrode, the lower-end ones (A1, A2, B1, B2) were discarded and selected as the most promising samples (C1, C2, D1, D2). In this case, two other types of ionic liquids were involved and added to the previous list ([Bmim] [NTf_2], [HMTA] [NTf_2]).

Gas chromatography unlike the Clark electrode allows to obtain much more accurate results and renders it possible to study in a more precise way the influence of each variable. The empty tests, conducted with only the presence of water and cerium ammonium nitrate, confirmed the absence of activity as theoretically expected (Figure 3.6).

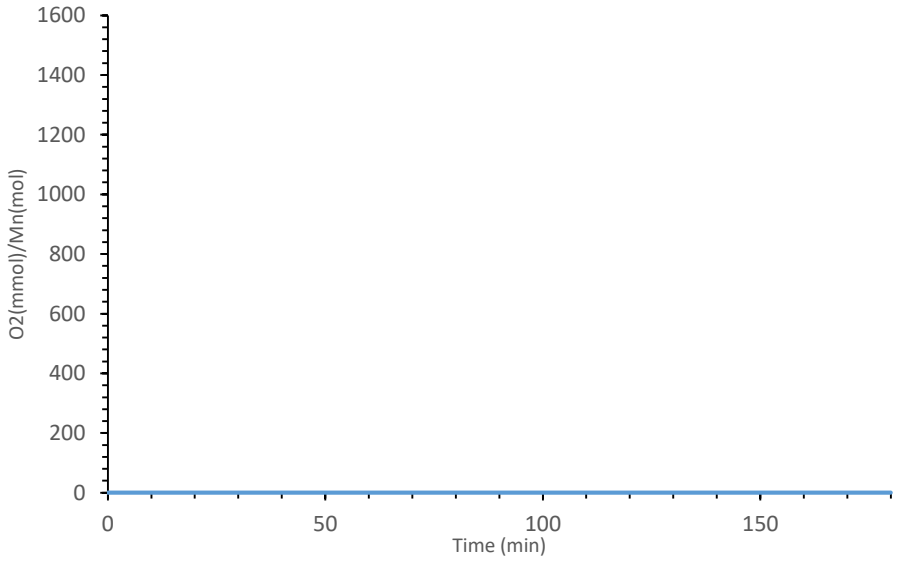

Figure 3.6 *The activity curve (in blue) demonstrate that reaction of water oxidation doesn't start without catalyst and with the only presence of Cerium ammonium nitrate.*

Furthermore, the amount of sample analysed was two times higher (2 mg), and, therefore, the result is more representative. Also, the timing on which the activity was monitored could be much more wide (3h instead of 10min) because with this measurement method there was not any problem of signal saturation.

3.3.1 Elaboration of data

In the vial, since the water phase was already saturated, the oxygen produced inside the liquid volume was flowing through the L-V interface to the headspace.

Data collected with the procedure explained in paragraph 2.2.2 consists of chromatograms that show two peaks, one proportional to the amount of oxygen and the other proportional to the amount of nitrogen (see example in Figure 3.7).

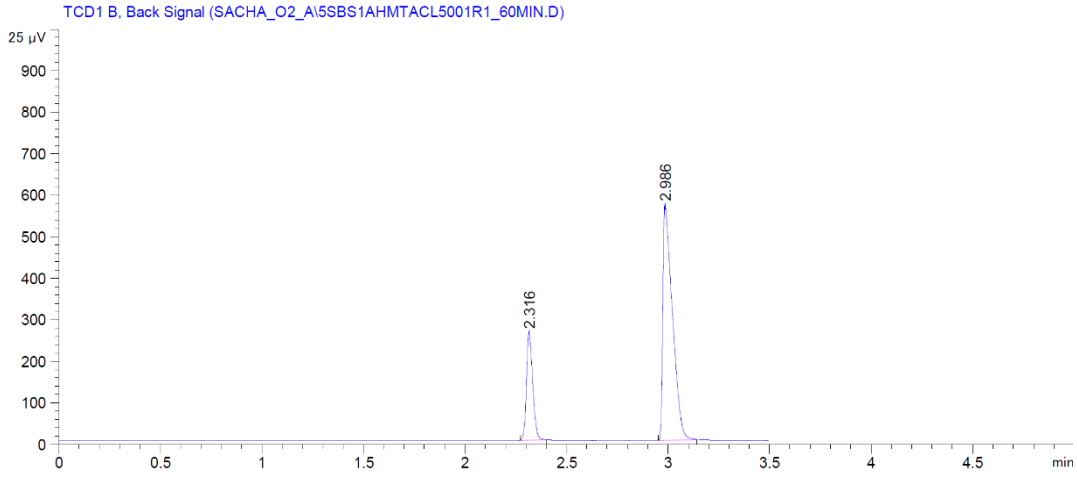

Figure 3.7 *An example of a chromatogram.*

Knowing the percent area of these two picks, allows us to calculate the amount of oxygen that was present in each time instant for a given sample. From that, we have built a series of curves expressed as: m-moles of O_2 produced vs. time.

Specifically, in order to convert the area percent of O_2 to moles of O_2, since the operative conditions was mild (40°C, ambient pressure), the ideal gas model was assumed to be valid:

$$P \cdot V = n \cdot R \cdot T \tag{3.5}$$

that inverted, results in:

$$n_{O_2} = \frac{P \cdot V}{R \cdot T} \tag{3.6}$$

and in this case:

- P is equal to 1 atm;
- $V = V_{Hs} * A\%_{O_2}$; with V_{Hs}=6.7*10^{-3} L (headspace volume) and $A\%_{O_2}$= percent area of the oxygen pick;
- R is the universal gas constant (0,08205784 $\frac{\text{atm·L}}{\text{mol·K}}$);
- T it has been assumed equal to the reaction temperature (usually 313.15K) but since that during analysis, the headspace was outside of the reactor bath, its

temperature was probably lower because of the dissipation. For this reason, the result show in this paragraph will be a little bit underestimated.

The first chromatogram of each measurement is a snap-shot of the situation after 10 min from the beginning of the reaction. At the time zero, the headspace contained just normal air atmosphere and so it was subtracted from the initial value of O_2 amount. This is fundamental in order to obtain the amount of oxygen produced. Thus, before the initiation of every analysis, the composition of ambient air was analysed in order to then exclude it from every snap-shot. Thus, we started every time from the value zero at time-instant zero.

Percent area of oxygen pick will be now express as:

$$\mathrm{A\%}_{O_2\ produced} = \mathrm{A\%}_{\mathrm{O_2}} - \mathrm{A\%}_{\mathrm{O_2,0}} \tag{3.7}$$

Anyway, in literature, gas-chromatography results are often expressed as mmol O_2/ mol Mn and so in this way to be able to compare the results between the different kinds of catalysts and different experiment procedures. Starting from only know that 2 mg of catalyst was used in each and every measurement, in order to normalize all the curves per moles of manganese, it was necessary run an ICP-OES analysis that allows us to find the amount of manganese as mg of catalyst (see Table 3.3).

Once the ratio was known, every point of each curve was recalculated as expressed in the follow equation:

$$\frac{n_{O_2}}{\frac{Mn_{ratio} \cdot 2mg}{MW_{Mn}}} \tag{3.8}$$

3.3.2 Analysis of the results and discussion

With the help of gas chromatography we, first of all, wanted to verify and reconfirm the results obtained with the Clark Electrode but also investigate the influence of the annealing treatment and higher concentrations of ILs.

Table 3.2 *Synthesis details of samples analysed by means of gas chromatography.*

Sample	Water (ml)	$Ca(NO_3)_2 \cdot 4H_2O$ (mg)	$MnCl_2 \cdot 4H2O$ (mg)	Ionic liquid (g)	Type of ionic liquid	NaOH 0,8M (ml)
0	17,5	472,3	791,64	0	/	2,5
0X	17,5	/	791,64	0	/	2,5
C1	17,3	472,3	791,64	0,2	[Bmim]Cl	2,5
C2	15,5	472,3	791,64	2	[Bmim]Cl	2,5
C3	11,5	472,3	791,64	6	[Bmim]Cl	2,5
C4	5,5	472,3	791,64	12	[Bmim]Cl	2,5
C4X	5,5	/	791,64	12	[Bmim]Cl	2,5
D1	17,3	472,3	791,64	0,2	[N-allyl-HMTA]Cl	2,5
D2	15,5	472,3	791,64	2	[N-allyl-HMTA]Cl	2,5
E1	17,3	472,3	791,64	0,2	[Bmim]NTf2	2,5
F1	17,3	472,3	791,64	0,2	[N-allyl-HMTA]NTf2	2,5

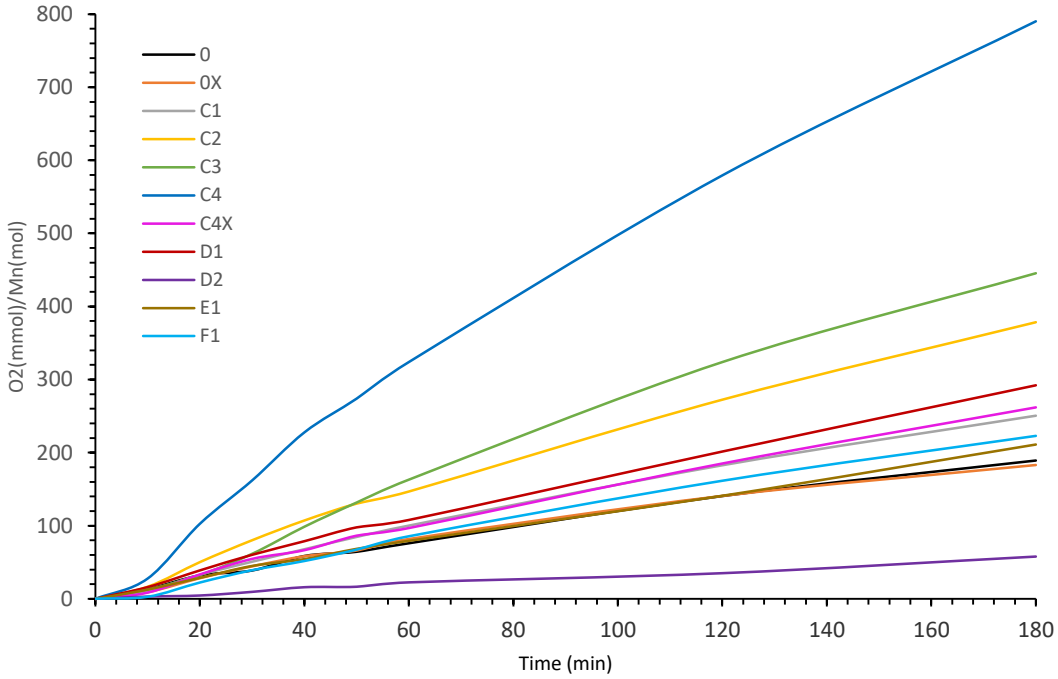

Figure 3.8 *Activity curves of different ionic liquids, at different concentrations.*

Figure 3.8 gives a standard overview of the sample activities starting when applying different ionic liquids, at different concentrations, before undergoing the annealing treatment (as reported in the previous paragraph with the Clark electrode).

This graph reconfirms the most of results observed previously. Calcium manganese oxide given birth with [Bmim] [Cl] is still the most promising water oxidation catalyst and the one from [N-allyl-HMTA] [Cl] is the second one. The IL concentration behaviour in terms of the activity is also consequent in both cases.

Nevertheless, also Figure 3.8 gives us interesting information. While there is a little difference between the activity curves of CaMnOx and MnOx synthesized with the hydrothermal method as already reported in the previous CE analysis, in the case of

gas chromatography, we observed a really large activity gap between the sample with the presence of calcium and the only manganese oxide both synthesized through iono-thermal procedure with a high concentration of [Bmim] [Cl] (respectively samples C4 and C4X where the first is the same in every point to the second except for the presence of Calcium). Therefore, the role of Ca and the loss of activity is expected, as reported in the literature but, in other hand, it became tricky to understand why through the iono-thermal method we obtained these results and while in case of the samples 0 and 0X (obtained by hydro-thermal synthesis), the gap is minimized.

The new two ionic liquids introduced in these tests ([Bmim] [NTf_2], sample E1; [N-allyl-HMTA] [NTf_2], sample F1), even if they lead to an increasing of O_2 production did not demonstrate a truly great potential.

If seeing Figure 3.8, we also see that how the IL concentration is in some way related to the activity as already reported in Figure 3.1. [N-allyl-HMTA] Cl concentration is inversely proportional compared to the total oxygen production while in case of [Bmim] [Cl] the opposite is true as confirmed by the test of four [Bmim] [Cl] concentrations (C1, C2, C3, C4), respectively, equal to 10, 100, 300, 600 mg/ml.

3.3.3 Annealing treatments

Annealing treatment is another important theme that we deal in this thesis. We wanted to understand whether and how much this process can influence the activity of our catalysts.

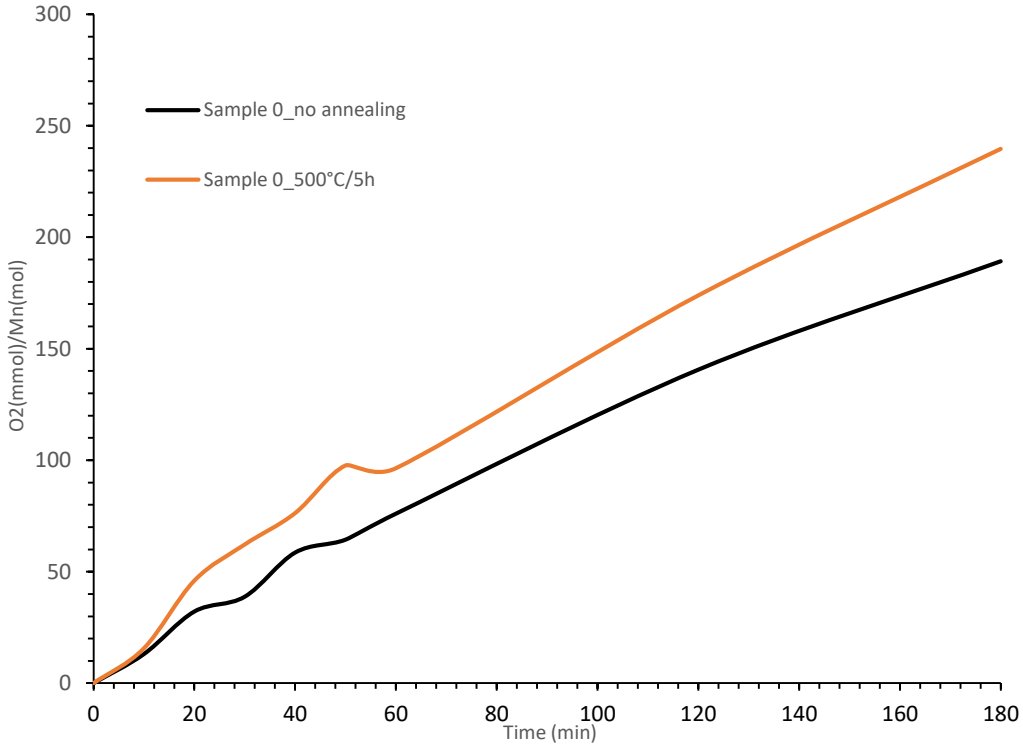

Figure 3.9 *The influence of annealing treatment recorded by GC.*

When observing Figure 3.9, the advantage obtained is obvious. The standard 0 after annealing is more or less 27% more active than the same sample but not treated. This means that when the catalyst is exposed to high temperatures sufficiently long times, a change occurred in the compound structure and maybe caused changes in its composition (it will be verified later in the characterization paragraph).

On the other hand, what is depicted in Figure 3.9, is only the results of a specific catalyst exposed to fixed operative conditions (temperature and time) of annealing but if we compared this same figure to the curves in Figure 3.3 (obtained by using different annealing temperature and time), we can observe how they can be altered. For this reason, different samples underwent different kind of temperature/time treatments.

For simplicity, let us consider only one sample. Figure 3.10 represents the influence of different heating conditions for the standard sample ‘’0’’.

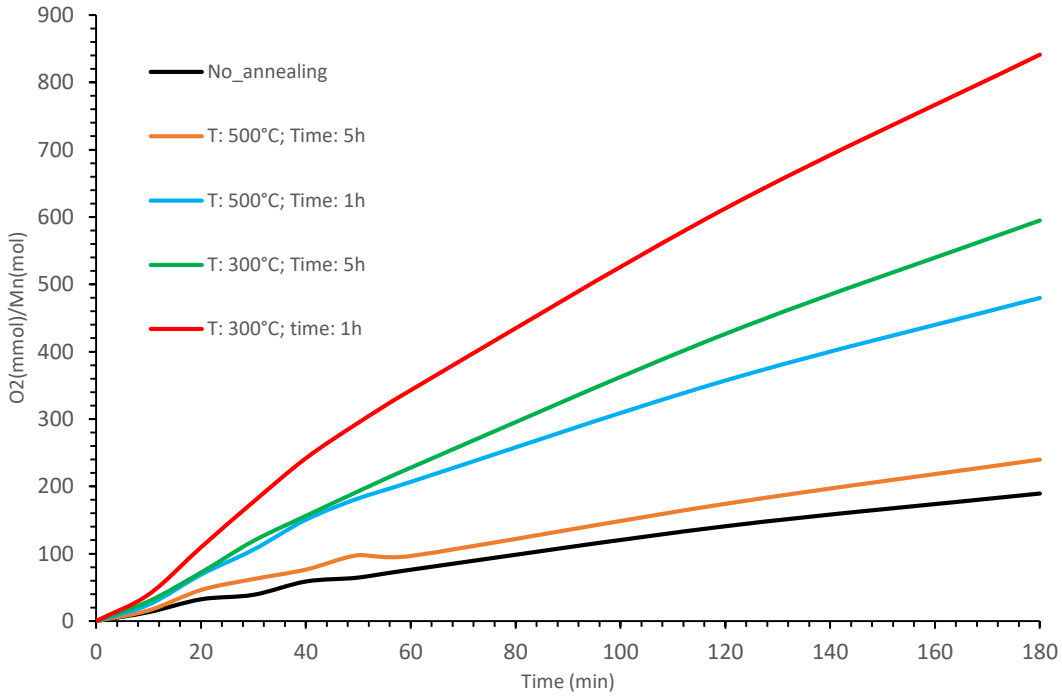

Figure 3.10 *The influence of different annealing conditions on the standard sample 0.*

Thanks to this observation, it become easy to conclude that high temperatures have somehow a negative effect on the catalysts activity. This could also explained why in Figure 3.3 we obtained a marked increment of O_2 production after annealing at 700°C. Regarding time, curves with a higher heating time give rise to a lower oxygen production. However, times shorter than 1 h and temperatures lower than 300°C revealed that a heterogeneous material was formed that was not completely annealed.

This trend is followed also by other samples, as you can depict in Figure 3.11. An exception is given by the relation existing between the activity and annealing conditions of the sample D1. This sample, treated at 500°C for 1h, shows a higher activity compared to the same sample treated at 300°C for 1h as well as all other cases.

The cause of this behaviour is probably due to the stability problems of the ionic liquid [N-allyl-HMTA] Cl and, to the fact, that high temperatures may favour a better combustion of the organic substances that contaminate this type of catalysts. In any case, this thread will be retaken on the next paragraph, where thanks to the

characterization tests, these assumptions will be verified.

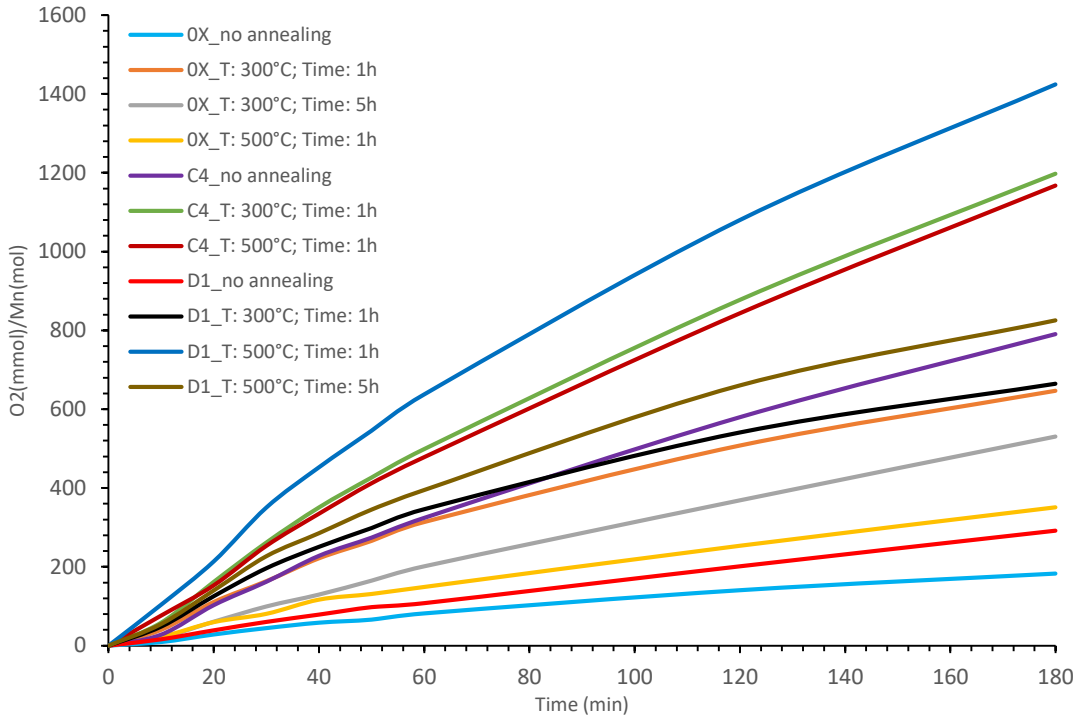

Figure 3.11 *The activity of different annealed catalysts.*

Generally, in a solid material exposed for long time at high temperatures, the molecules have time to arrange themselves in a more orderly way by forming a crystal lattice. Said that, the results displayed in Figure 3.11 tell us how in the case of water oxidation reaction an amorphous catalyst it will be more efficient than a crystalline one.

With this concept in mind, all the other samples were calcined at the lowest annealing temperature and the shortest time as illustrated in Figure 3.12. Sample C4 still remains the best performing one.

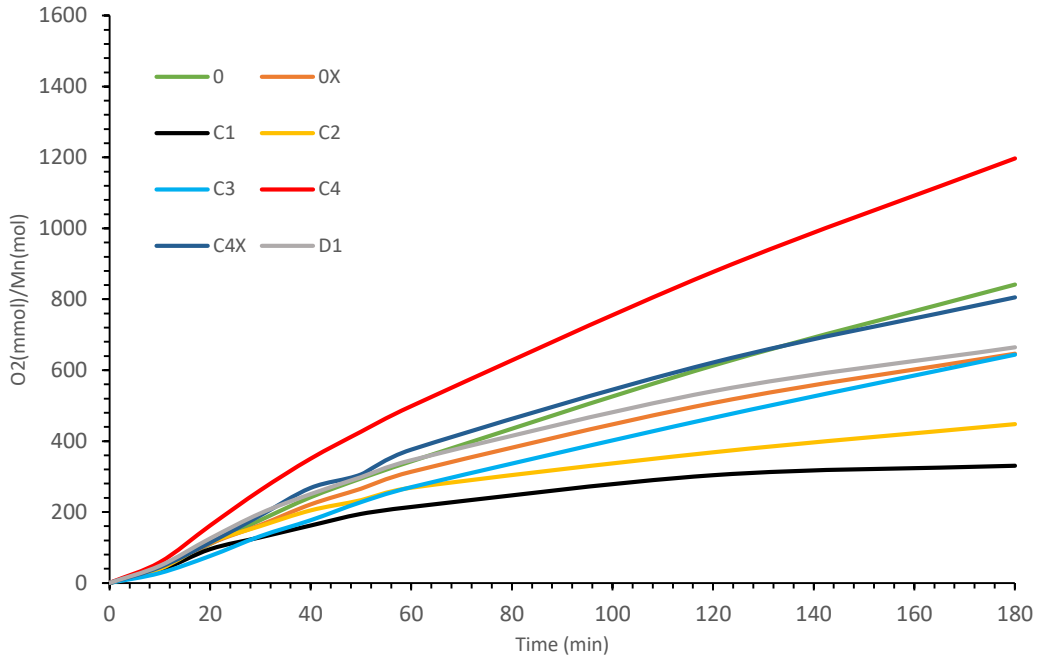

Figure 3.12 *Comparison between standards and most promising sample annealed at 300°C for 1 hour.*

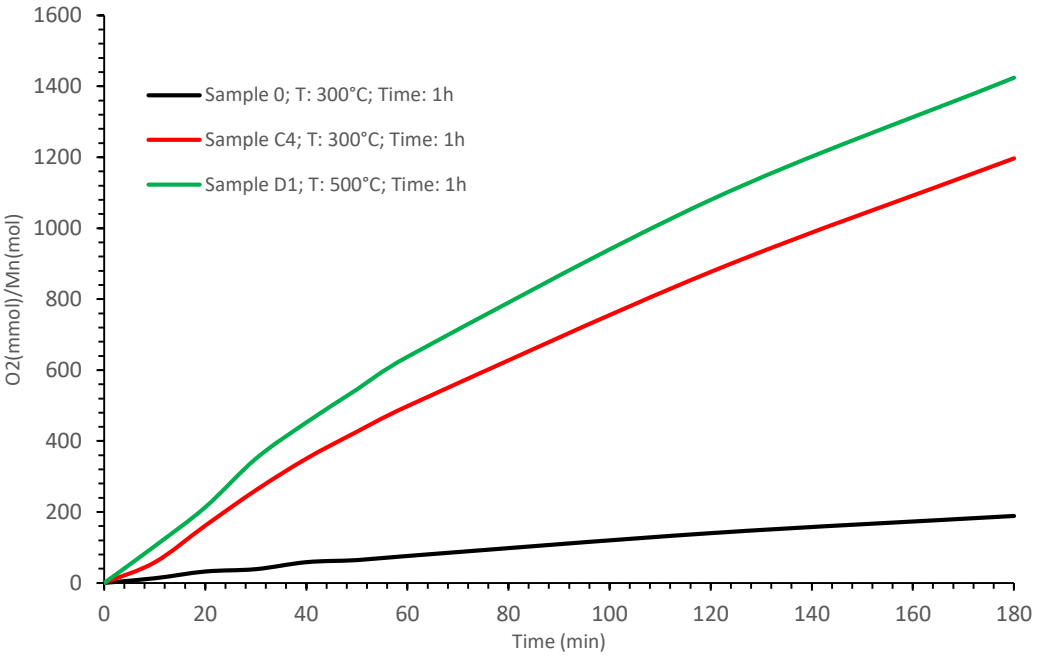

Figure 3.13 *Comparison between best sample at optimal synthesis conditions and standard sample.*

3.3.4 Catalyst lifetime

The lifetime of a catalyst is an another important feature of industrial catalysts since it is crucial in terms of its feasibility.

With this idea, a sample used in a measurement for the first time, was washed, centrifuged and analysed the second time. The loss of activity reported in Figure 3.14 is not negligible and, indeed, it seems to indicate a poisoning phenomenon or changes in the x structure of the active sites. The first hypothesis seems to be more plausible since after washing and centrifugation of the 2 mg of sample analysed, the total weight was increased with more or less 150%.

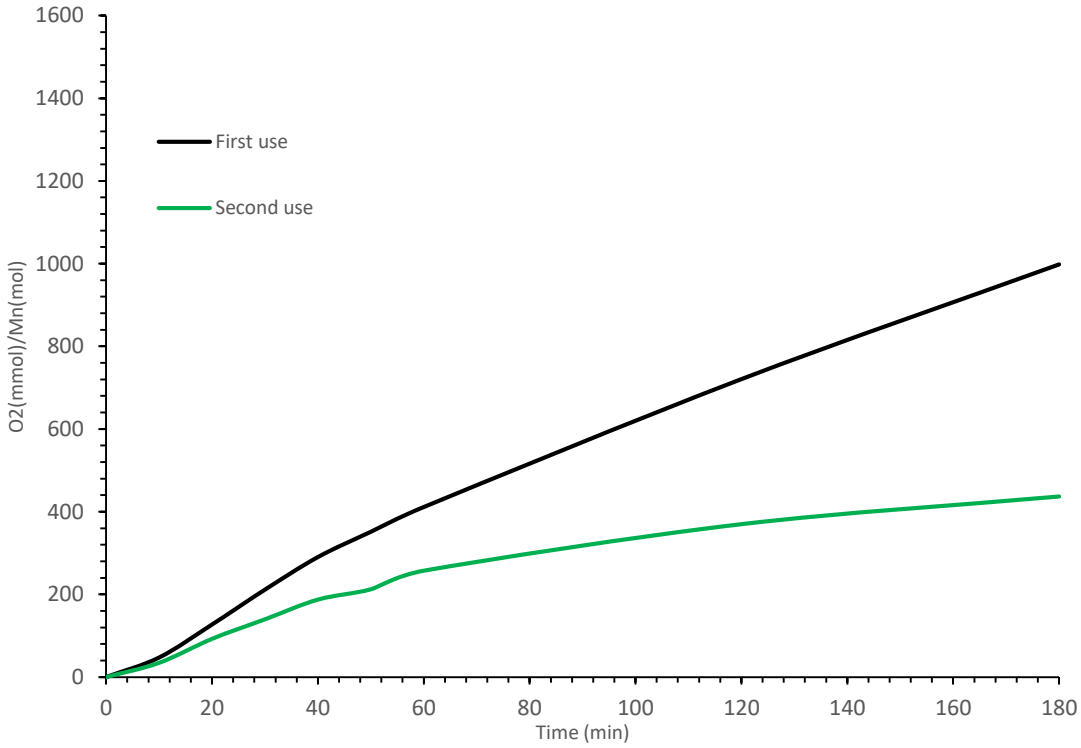

Figure 3.14 *Life-time test. The catalyst after the first cycle of 3 hours loses almost 50% of its activity.*

3.3.5 Reactor temperature

Lastly, but not less important, the reaction conditions play a significant role in terms of the total yield. In particular, we investigated temperature influence on the kinetics of water oxidation reaction. Figure 3.15 gives an overview of the three activity curves obtained by running test with the same type of catalyst, at three different temperatures of the oil bath (40°C, 60°C, 80°C). Given that this reaction is lightly endothermic, the results reflect the theoretical expectations (80°C curve gives after 180 min almost two times better results that the one performed at 40°C).

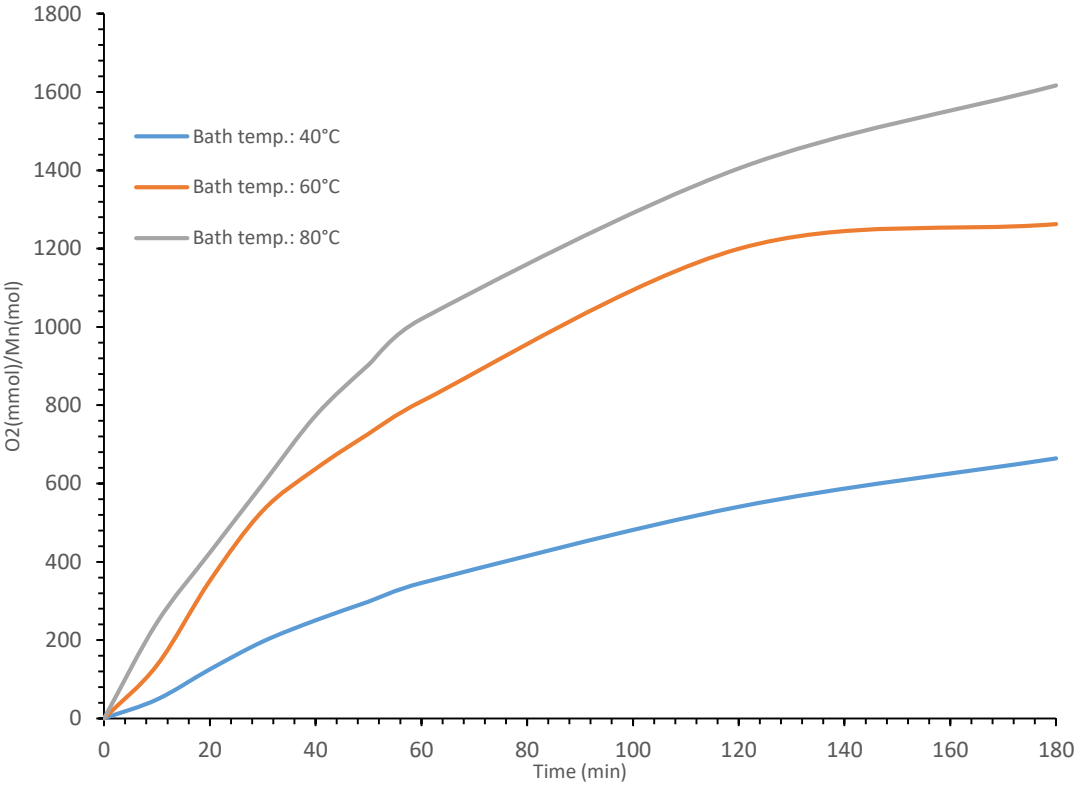

Figure 3.15 *Sample D1 annealed at 300°C for 1 hour and tested at three different temperatures.*

Regarding the pressure, as dictate by Equation 1.3, we note how from reagents to products of the number of moles is increasing. This means that a decrease in pressure promotes an increase of oxygen production. Opposite, instead, should be theoretically the effect following to an increasing of pressure. Anyway these considerations have not been proved yet by experimental test.

3.4 Activity tests: CV/LSV

CV/LSV, allows for measuring the activity and the determination of the over-potential or, rather the potential which is necessary to apply in order to initiate the water splitting reaction.

The activity tests carried on with this technique unfortunately did not reveal any new information, since troubles were encountered upon the carbon electrode preparation (explained in paragraph 2.2.3):

- **Higher amount of Nafion ⇒ higher stability but lower activity (less current) of the electrode.** Indeed, Nafion creates a conductive layer that keeps

together the catalyst (usually metal oxides are isolators) but, at the same time, this layer doesn't allow a direct contact of catalyst with reagent (water) and so it inhibits the catalytic action.

- **Lower amount of Nafion ⇒ lower stability.** It's easy losing some catalyst inside the cell.
- **Less catalyst on the electrode ⇒ lower activity.** Less catalyst means less active sites are available.
- **Too much catalyst on the electrode ⇒ lower activity.** Because of the scarce conductivity of metal oxides such as MnOx and CaMnOx, the layers that form on the electrode if too thick, can isolate the carbon electrode.

As a result, no reliable and comparable measurements could be conducted since the results were dependent on the choices made during the deposition procedure of the sample on the electrode.

An example, (Figure 3.16) the same sample prepared in two different ways exhibited different activity almost equal to one order of magnitude.

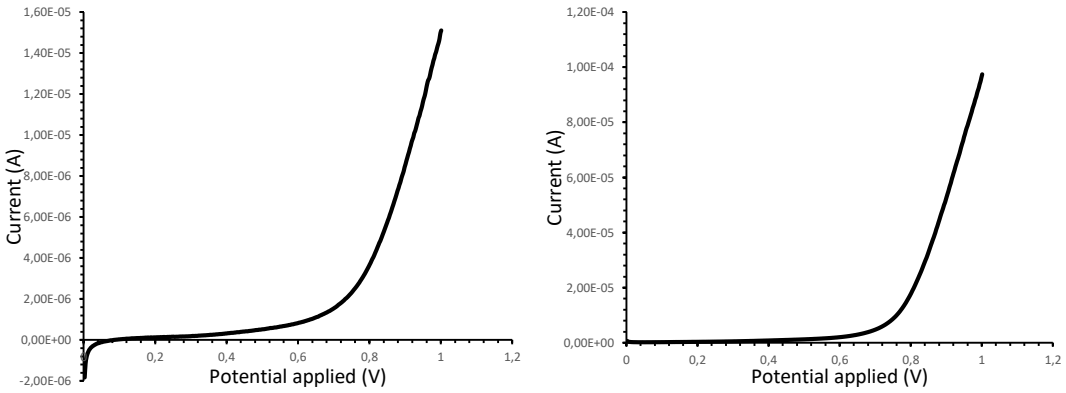

Figure 3.16 *Comparison between different results obtained from the same sample but with another electrode deposition method.*

3.5 Characterization of a selected group of compounds

Among all the compounds synthesized, only few samples were selected as most active or of scientific interest for special aspects. In the next subsections will be described some observed features of the selected catalysts that were subject to various characterization analysis mentioned in the previous chapter.

3.5.1 Scanning Electron Microscope

Even if the Scanning Electron Microscope doesn't measure a specific feature of a material, it gives an external overview of the sample that in this case correspond with its crystalline/amorphous structure. The understanding of the surface shape coupled with other characterization and activity analysis results could be really helpful for the verification of some hypothesis.

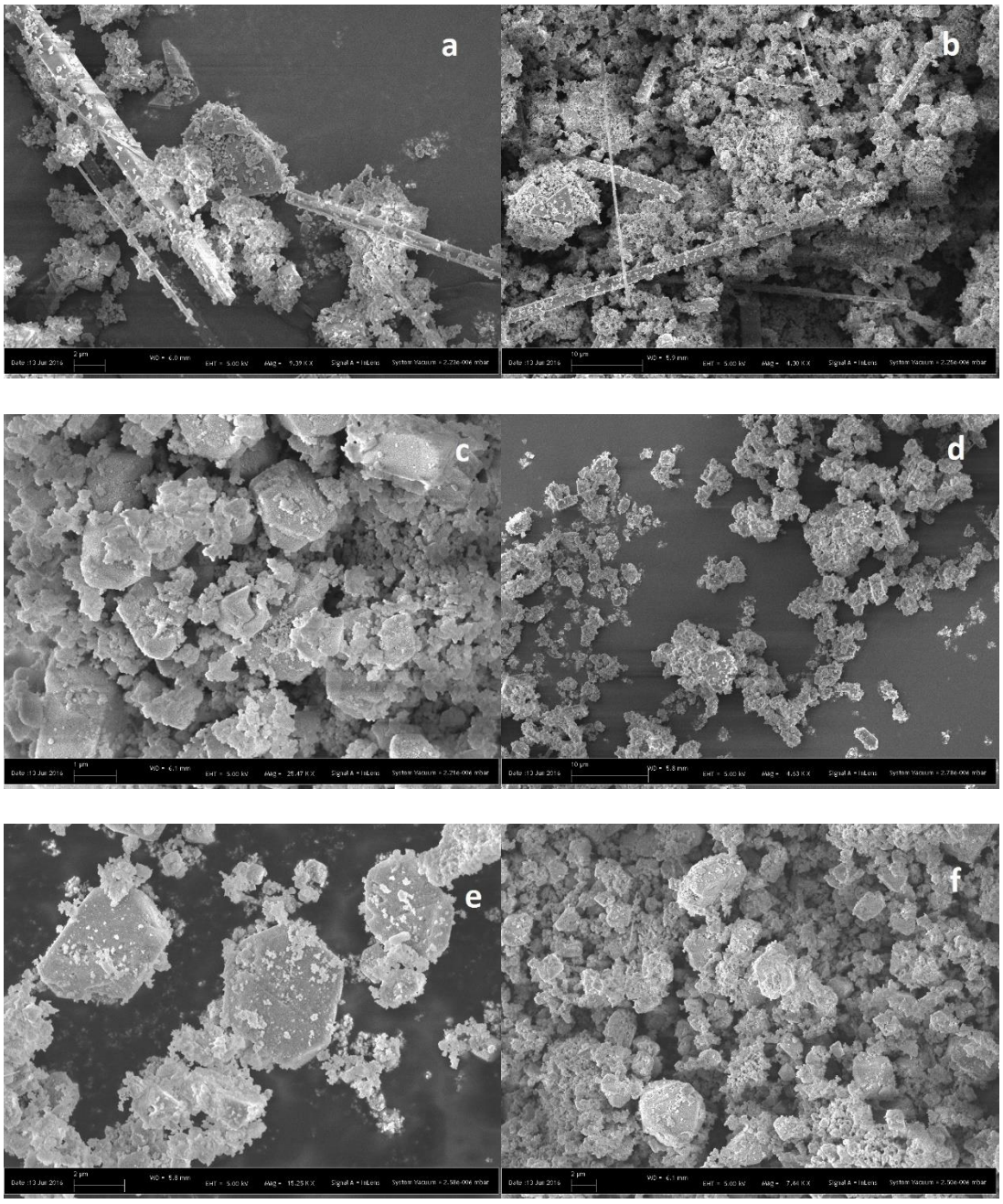

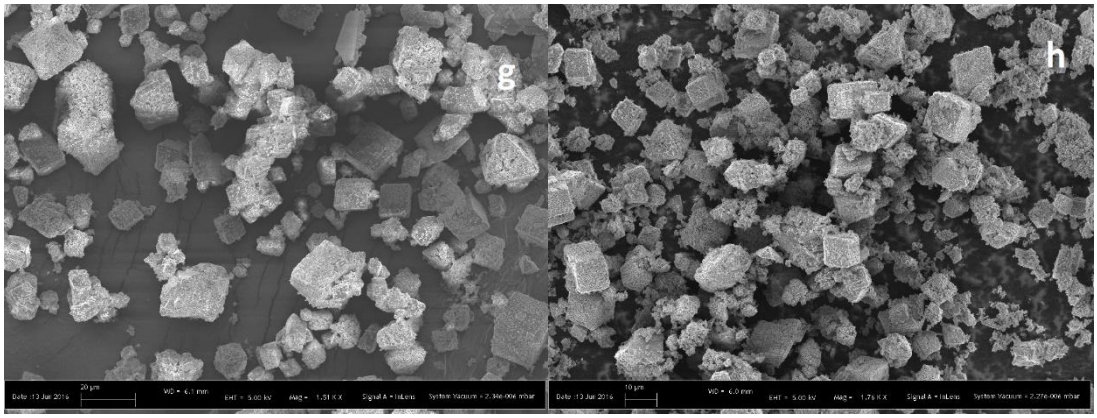

Figure 3.17 *SEM pictures: (a) sample 0 before annealing; (b) sample 0 annealed at 300° for 1h; (c) sample 0X annealed at 300° for 1h; (d) sample C4 before annealing; (e) sample C4 annealed at 300° for 1h; (f) sample C4X annealed at 300° for 1h; (g) sample D1 before annealing; (h) sample D1 annealed at 300° for 1h.*

Note that when observing these images, we see how a change in the ionic liquid leads to a considerable alteration of the crystalline structure and its amount (respect to the amorphous one). In the absence of an ionic liquid (Figure 3.17 pictures *a* and *b*), the catalyst structure seems composed mostly of an amorphous phase mixed with rods shape crystal while in the presence of it, in case of [Bmim] [Cl], the sample seems totally amorphous (Figure 3.17 pictures *d*, *e* and *f*) and with [N-allyl-HMTA] [Cl] (Figure 3.17 pictures *g* and *h*) appears a ‘’pseudo-cubic’’ crystalline shape.

Secondly, the majority of samples highlight the presence of mesoporosity that is an essential property in a good chemical catalyst. Anyway this feature will be verified and quantified thanks to the nitrogen physisorption analysis.

3.5.2 Inductively Coupled Plasma Optical Emission Spectrometry

In literature, in order to compare the results coming from different catalysts, all scientific articles generally normalize all curves dividing them for the mole manganese contained in the sample (we will call this property the specific activity). Explained in other words, manganese has been taken as a reference to identify the real quantity of active sites present in a specific amount of powder.

Furthermore, ICP-OES can be useful for determine, on a surface and in the bulk of a particle, the calcium amount that, as said in Chapter 1, could play an important role in the water oxidation catalysis.

Table 3.3 reports the results and it shows two important contradictory facts regarding calcium. Firstly, Ca is present in a minimal amount in all samples while secondly, the MnOx samples revealed its presence even if it was not used as a precursor during the synthesis process.

Table 3.3 *ICP-OES analysis results.*

Sample	Annealing	Ca/Catalyst (mg/mg)	Mn/Catalyst (mg/mg)
0	no	0,004433645	0,30558945
0	300°C; 1h	0,004802353	0,313530148
0X	300°C; 1h	0,004488806	0,341723672
C1	300°C; 1h	0,004513501	0,358214752
C2	300°C; 1h	0,005446755	0,344509804
C3	300°C; 1h	0,005878859	0,311816531
C4	no	0,009639374	0,274580692
C4	300°C; 1h	0,011710441	0,348439085
C4X	300°C; 1h	0,003834268	0,32324978
D1	no	0,004559659	0,278051118
D1	300°C; 1h	0,007330853	0,307077803
Ca/Mn Ratio=1/1	no	0,003934633	0,321500476
Ca/Mn Ratio=1,5/1	no	0,003416677	0,358680269
Ca/Mn Ratio=2/1	no	0,003610953	0,336294626
All chloride precursors	no	0,006097638	0,367486902
Blank test	/	0,006547898	-0,006679296

To overcome this experimental problem, two strategies were chosen:

- changing the Ca/Mn precursors ratio;
- using $CaCl_2$ instead of $Ca(NO_3)_2 \cdot 4H_2O$;

as shown in Table 3.3, neither an increase in the precursor amount nor the use of the same anion in the starting salt, resulted in an increase in Ca concentration in the final product. Probably, this inconsistency resides in the procedure itself and the only way for obtain a higher content of Ca is to use another preparation method, not the classical precipitation procedure. However, note that a higher concentration of an ionic liquid, allows bonding more Ca to the precipitate (probably thanks to the strong ionic interactions).

On the other hand, Ca was found in a sample where calcium wasn't expected taking into account that the manganese oxide should contain only manganese and oxygen. Initially, the reason seemed to be or a contamination in the powder of the manganese salt or an autoclave contamination. Therefore, a new commercial batch of $MnCl_2 \cdot 4H_2O$

was purchased and at the same time it has carried out a prewash of the autoclave with hydrochloric acid (37%w/w) in order to remove any possible calcium contamination was applied. Nevertheless, the hypothesis was not supported. Fortunately, after several attempts, a blank analysis on the carrier liquid used for ICP-OES revealed the real cause. Indeed, was found that the same amount of Ca was analysed in the blank test and the MnOx sample test. This can only mean that Calcium recorded originates from the Millipore water used with HCl as the carrier liquid. The Raman spectra of the sample 0X reported in Figure 3.18, confirms the presence of the typical peak that represents the Mn_3O_4 bonds (~656 cm^{-1}) only [63].

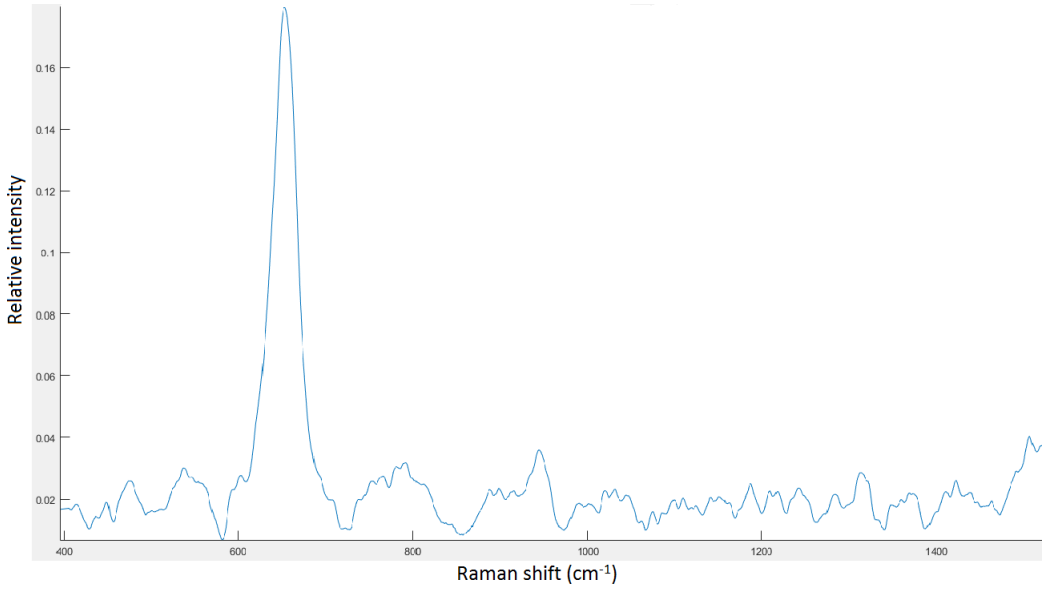

Figure 3.18 *Raman spectra of sample 0X shows a dominant peak typical of Mn_3O_4 (~656 cm^{-1})* [63].

3.5.3 Volumetric Nitrogen absorption

One of the aims of this study is to demonstrate that ionic liquids, thanks to their steric hindrance and their strong interaction forces, are able to coordinate the synthesis of the oxide structure in a way that, after the washing step, ionic liquid trapped between solid molecules of CaMnOx is washed out and so it should form large mesoporous in the catalyst particle structure.

According to what it was just reported, an analysis of nitrogen physisoption measurements were carried out for the most promising samples. Morphological

characteristics of interest are surface area, pore volume, area and pore size distributions[59]. The results are shown in the following table:

Table 3.4 *Nitrogen physisorption analysis results.*

Sample	Annealing	BET area (m2/g)	Pore size (nm)	Pore volume (cm3/g)
0	no	6,8563	15,97644	0,027385
0	300°C; 1h	11,3375	21,97691	0,062291
0X	300°C; 1h	35,8007	26,25447	0,234982
C1	300°C; 1h	30,9356	32,0792	0,248097
C2	300°C; 1h	31,2529	46,28963	0,361672
C3	300°C; 1h	31,3735	71,2486	0,558565
C4	no	10,741	19,81322	0,053204
C4	300°C; 1h	44,5547	32,49222	0,36192
C4X	300°C; 1h	32,8917	59,68162	0,490758
D1	no	2,9581	28,62975	0,021173
D1	300°C; 1h	31,3545	32,24202	0,25733

In general, the pore texture arises from the preparation methods of these solids [59]:

- precipitation from a solution originates from the precursor particles that agglomerate for a porous structure;
- Hydrothermal and specially iono-thermal crystallization produces zeolites or other crystalline microporous compounds, where the peculiar arrangement of the ‘’building units’’ generates intra-crystalline cavities of molecular size;
- elimination of volatile materials during thermal treatments (burning, evaporation) produces cavities as the result of both solid rearrangement and exit way of the removed material.

These three points and initial hypothesis were proved as reported in Table 3.4:

1. The precipitation method and the iono-hydrothermal crystallization used for the synthesis of all samples form a porous material;
2. Annealing treatment gave rise to a B.E.T. surface area almost two times higher in the case of sample 0, more than four times in the case of C4 and even almost ten times in the case of sample D1. This last fact demonstrates how the sample D1, even if it contained a low concentration of an IL, is strongly contaminated because of the decomposition of cation [N-allyl-HMTA]$^{+}$ and by burning it at high temperatures (annealing at 300°C or better 500°). This contamination flies out, leaving free space and creating a wide network of pores.

3. The presence of ionic liquid gives a gain in the sense of activity. Already the samples C1 and D1, even if synthesized in a solvent with a minimal concentration of ionic liquid (10g/l), gave rise to a significant improvement (reported in Table 3.4) in terms of porosity.
4. An increasing of IL concentration is equivalent to an increasing porosity. An ILs acts, at the same time, as a solvent as well as template for the building of a specific porous structure depending on the IL type employed.

High surface area is not the only important feature for a catalyst in this kind of analysis. In fact, two catalysts with the same way of synthesis, composition, structure and especially surface area, can have two different activities. This could happen because of the porosity typology. The pores are classified in different classes depending on their size [59]:

- micropores (size <2nm), ultramicropores (size <0.7nm);
- mesoporous (2nm<size<50nm);
- macropores (size>50nm).

A catalyst which is mostly containing mesopores and macropores will be more active than an identical one but formed mainly by micropores or ultra-micropores. The reason is that, in many cases, the reagents of a reaction are not able to penetrate and take advantage of the active sites present inside micro/ultra-micropores or too much time is required to reach and leave them. In this way, a large part of surface area is not exploited properly and it remains unused.

Normally, what you prefer in a porous catalyst, is the mesoporosity as it is the right compromise between the total volume occupied in relation to its surface and the vacuum degree necessary to facilitate the passage of the reactants through the pores.

Referring now to the curve in Figure 3.19 that we have obtained for sample C4 and that follows the trend of the most of the other samples, we notice the existence of hysteresis. As he explained in the second chapter the presence of hysteresis in the curves of adsorption and desorption, testify the presence of mesoporosity. This is also reported in Table 3.4 from the sizes of pores in reference to what above described on the types of existing pores.

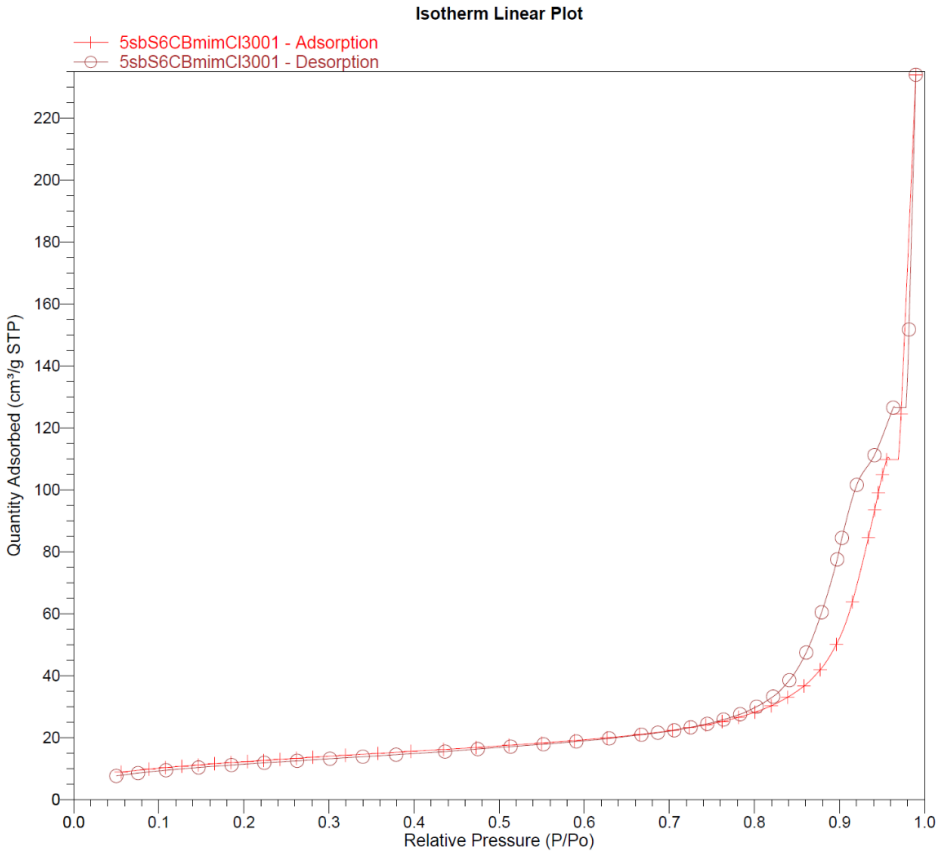

Figure 3.19 *Nitrogen adsorption/desorption of sample C4 annealed at 300° for 1h.*

3.5.4 X-ray Photoelectron Spectroscopy

Referring to what has been said in paragraph 2.3.4, the active zone of a catalyst is its surface and so, independently from the composition or structure assumed by the bulk there is no influence on the activity.

Table 3.5 reports the percentage amounts of the main elements that catalyst is constituted of.

First of all, we note how the manganese amount was recorded, and confirm the results obtained upon the ICP-OES analysis. Secondly, another important result is the oxidation state that manganese assumes in each sample: for all the samples before annealing, it is almost equal to 50% MnII and 50% MnIII while in other cases (annealed), it is equal to +3 as in the OEC complex (which is what we want mime). The annealing treatment proves to be a fundamental step to obtain an efficient catalyst.

Another important consideration can be noted in terms of the amount of cerium revealed in lifetime sample after a first use. Cerium has been found on the surface with a percentage of 8,18% against the 3,91% of manganese. This can only mean, that Ce is a poison for the catalyst and during the reaction it attached permanently on the active sites of the catalyst by inhibiting it. As already explained in the first chapter, all of activity test (apart for CV/LSV) were carried out with Ce ammonium nitrate as the oxidant agent since among all choices it is the one that doesn't release oxygen (unlike from H_2O_2 or others). This feature becomes fundamental if we want to measure the oxygen produced – otherwise the results would be dependent also from the decomposition kinetics of the oxidant agent.

An observation is also the high carbon amount found in every sample. Carbon is an inert from the point of view of water oxidation catalysis and for this reason we don't need its presence in the compound. However, percentages even close to the 50% were recorded, especially for samples not annealed (as expected since that keeping samples at high temperature lead to burn a part of carbon contamination). This weird result can only be caused by a contamination that can be attributable to three different factors during the synthesis process:

- the autoclave used has a PTFE core that if heated at operating temperature (180°C) could release some carbon (T_g=115°C, T_m=327°C);
- the drying of sample was carried out by placing samples in a plastic (PP, T_g=0°C, 130°C<T_m<171°C) tubes for then putting and keeping them inside an oven for ~16h at 80°C/100°C. this can lead to a contamination of the sample in contact with the wall of tube;
- air pollution. It is known that XPS is a really sensitive instrument, prolonged exposure to air of the sample could lead to its contamination (even if it couldn't justify so high an amount).

With the aim to discover the cause of this issue, a point-by-point exclusion procedure was applied: the main contribution of carbon comes exactly from the plastic tubes used during the drying treatment. This fact was proven by the sample dried in a glass tube instead of a plastic one. See Table 3.5 with the name of ''*Glass 0*'' that displays a substantial decrease in the carbon content (11.82% against the

30.04% of the equivalent sample ‘’*0*’’). The percentage of carbon still present could be attributed to the other two hypotheses.

Table 3.5 *XPS results show the composition % (BDL= below detection limit) and the oxidation states of manganese inside each sample.*

Sample	Annealing	Mn %	Ca %	C %	O %	Ce %	Mn Ox.state
0	no	24,06	BDL	30,04	45,89	0	Mn(III)+Mn(II)
0	300°C; 1h	29,89	BDL	19,74	50,36	0	Mn(III)
0X	300°C; 1h	36,96	BDL	10,92	52,14	0	Mn(III)
D1	no	22,49	BDL	28,79	44,53	0	Mn(III)+Mn(II)
D1	300°C; 1h	33,47	BDL	15,63	50,91	0	Mn(III)
C4	no	25,87	traces	23,34	42,78	0	Mn(III)+Mn(II)
C4	300°C; 1h	32,11	2,18	13,38	49,8	0	Mn(III)
Lifetime 1	300°C; 1h	32,11	2,18	13,38	49,8	0	Mn(III)
Lifetime 2	300°C; 1h	3,91	BDL	51,67	36,23	8,18	Mn(III)
Glass 0	no	32,92	BDL	11,82	42,48	0	Mn(III)+Mn(II)

Lastly, note that the large difference on the calcium amount between C4 and 0 can easily explain why in the activity tests analysed with a GC, we observed a large gap from C4 to C4X (as expected because of the role of calcium) and not confirmed from the one between 0 and 0X.

3.6 Modelling of a reaction kinetic law

As introduced in the first chapter, the reaction of water splitting can be write as a sum of its two half-reactions:

Total reaction: $$H_2O \rightarrow H_2 + \frac{1}{2} O_2 \quad (3.9)$$

Water reduction: $$2\ H^+ + 2\ e^- \rightarrow H_2 \quad (3.10)$$

Water oxidation: $$H_2O \rightarrow \frac{1}{2} O_2 + 2\ H^+ + 2\ e^- \quad (3.11)$$

Calcium manganese oxide catalyses the oxidation half-reaction.

When observing the curves obtained in GC tests and since that water oxidation involves only one reagent (H_2O), we can assume a first order kinetic behaviour that can be described it through the general equation:

$$R = K \cdot C_{H_2O} \tag{3.12}$$

where R is the reaction rate $\left(\frac{mmol}{L \cdot min}\right)$, K is the kinetic constant, expressed in this case as min^{-1} and C_{H_2O} the concentration (mM) of the reagent water. As a consequence, the production/consumption rates (r) of each species involved is given by the following equation:

$$r = \nu_i \cdot R \tag{3.13}$$

with ν_i is the stoichiometric coefficients of the species *i* and where *r* can be express also as:

$$r = -\frac{dC_{H_2O}}{dt} = 2\frac{dC_{O_2}}{dt} = \frac{dC_{H_2}}{dt} \tag{3.14}$$

Combining Equation 3.13 with 3.11 and 3.14 and assuming the irreversible reaction, isothermal conditions and a constant density, the material balance of each single species for the batch system can be written as the differential equations reported below:

$$\frac{dC_{H_2O}}{dt} = -KC_{H_2O} \tag{3.15}$$

$$\frac{dC_{O_2}}{dt} = \frac{1}{2}KC_{H_2O} \tag{3.16}$$

$$\frac{dC_{H_2}}{dt} = KC_{H_2O} \tag{3.17}$$

If now, we would obtain the analytical expression that gives the concentration of Oxygen at a generic time instant C_{O_2}(t), Equation 3.16 has to be integrated:

$$\int_{C_{O_2,0}}^{C_{O_2,t}} dC_{O_2} = \int_0^t \frac{1}{2}KC_{H_2O}dt \tag{3.18}$$

by integrating Equation 3.15 we obtain:

$$\int_{C_{H_2O,0}}^{C_{H_2O,t}} \frac{dC_{H_2O}}{C_{H_2O}} = -\int_0^t K dt \tag{3.19}$$

$$\ln \frac{C_{H_2O,t}}{C_{H_2O,0}} = -Kt \tag{3.20}$$

$$C_{H_2O,t} = C_{H_2O,0} \cdot e^{-Kt} \tag{3.21}$$

As the next step, after inserting 3.21 in 3.18, we get:

$$\int_{C_{O_2,0}=0}^{C_{O_2,t}} dC_{O_2} = \int_0^t \frac{1}{2} K C_{H_2O,0} \cdot e^{-Kt} dt \tag{3.22}$$

$$C_{O_2,t} = -\frac{1}{2} K C_{H_2O,0} \frac{e^{-Kt}}{K}\Big|_0^t = -\frac{1}{2} C_{H_2O,0} \cdot e^{-Kt} + \frac{1}{2} C_{H_2O,0} \tag{3.23}$$

$$C_{O_2,t} = \frac{1}{2} C_{H_2O,0}(1 - e^{-Kt}) \tag{3.24}$$

Equation 3.24 represents the function that describes kinetically all the activity curves recorded during the analysis and, therefore, the production trend of oxygen over the time for each catalyst and it depends from the initial concentration of water and from the constant *k* characteristics for each and every catalyst.

Now, in order to find the characteristic kinetic constant (*K*) for each catalyst synthesized, a script in Matlab was created that was able to solve the material balances of the system and then finding the optimum *K* that gave the best fit to the experimental points. This code is structured as follows:

- As first part, all the parameters are declared:

```
 function ode_fitting
clc
clear all
format long
%H2O-->2H++0.5O2
k0=ones(1,27);                    %guess value matrix
nu=[-1,2,0.5];                    %stoichiometric coefficients
CIN=[0.056*1e6,0,0];              %mmol/L
CO2exp=load('CO2exptable');       %experimental data loading
texp=[0, 10, 20, 30, 40, 50, 60, 120, 180];  %min
```

- A second part where material balances are solved and the object function to minimize is calculated (relative error between experimental and calculated point):

```
function err= fob(par,CO2exp,tau,nu,CIN)
        sol=ode15s(@BM,[0 max(tau)],CIN,[],par,nu);
Ccal=deval(sol,tau);
err=norm((CO2exp'-Ccal(3,:)));
end

    function Cprimo= BM(tau, c,k,nu)
        R=c(1)*k;
        r=nu*R;
        Cprimo=r';

    end
```

- And lastly a third part where the objective function above defined is minimized for each catalyst tested:

```
for p=1:27
k(p)= fminsearch(@fob, k0(p), optimset('Tolfun',1*10^-10,'TolX',
1*10^-10, 'MaxIter', 10000), CO2exp.CO2exptable(:,p), texp,nu,CIN);
sol1=ode15s(@BM,[0 max(texp)],CIN,[],k(p),nu);
figure(p)
 plot(texp,CO2exp.CO2exptable(:,p),'bo',sol1.x,sol.y(2:3,:),'-
'),title(sprintf('k=%d [min^-1]',k(p)))
legend('O2exp','H+calc','O2calc'), xlabel('Time [min]'),
ylabel('Conc [mmol/L]')
end
```

The results gotten from this script have been then verify with the ones directly obtained from analytical solution:

```
for p=1:27
k(p)= fminsearch(@BMO2, k0(p), optimset('Tolfun',1*10^-10,'TolX',
1*10^-10, 'MaxIter', 10000), t, CO2exp.CO2exptable(:,p),CIN,nu);
CO2c=nu*CIN*(1-exp(-k(p)*t));
end

function fob = BMO2 (k, t, CO2exp,CIN,nu)
CO2calc=nu*CIN*(1-exp(-k*t));
fob=norm((CO2exp-(CO2calc'*1000))/CO2exp);
end
```

Values of *K* are reported in Table 3.6.

Table 3.6 *K values resulted from Matlab script.*

Sample	Annealing	K (1/min)	Sample	Annealing	K (1/min)	Sample	Annealing	K (1/min)
0	no	2,24E-07	C1	no	3,43E-07	C4X	no	3,14E-07
0	300°C; 1h	1,01E-06	C1	300°C; 1h	5,48E-07	C4X	300°C; 1h	1,04E-06
0	300°C; 5h	7,04E-07	C2	no	4,95E-07	D1	no	3,02E-07
0	500°C; 1h	5,88E-07	C2	300°C; 1h	6,74E-07	D1	300°C; 1h	8,54E-07
0	500°C; 5h	2,94E-07	C3	no	5,13E-07	D1	500°C; 1h	1,73E-06
0X	no	2,48E-07	C3	300°C; 1h	7,67E-07	D1	500°C; 5h	1,04E-06
0X	300°C; 1h	9,05E-07	C4	no	8,33E-07	D2	no	5,73E-08
0X	300°C; 5h	6,80E-07	C4	300°C; 1h	1,59E-06	E1	no	2,80E-07
0X	500°C; 1h	4,72E-07	C4	500°C; 1h	1,55E-06	F1	no	2,30E-07

3.6.1 Temperature dependence

In kinetics, the temperature dependence of the constant (*K*) and thus of the reaction rate, is conveniently expressed by the Arrhenius equation:

$$K = Ae^{-\frac{E_a}{RT}} \tag{3.25}$$

where *A* is the pre-exponential factor, *T* absolute temperature, *R* the universal gas constant and E_a the activation energy for the reaction.

Thanks to the tests carried on at different temperatures (40°C, 60°C, 80°C), one of the most active compounds (C4) (see 3.3.5), the calculation of the Arrhenius parameters (*A* and E_a) was feasible.

Starting from these three curves, the algorithm (describe above) was exploited to obtain the three different *K* values. Afterwards, the kinetic constants were plotted in a graph *ln K vs 1/T* (see Figure 3.20).

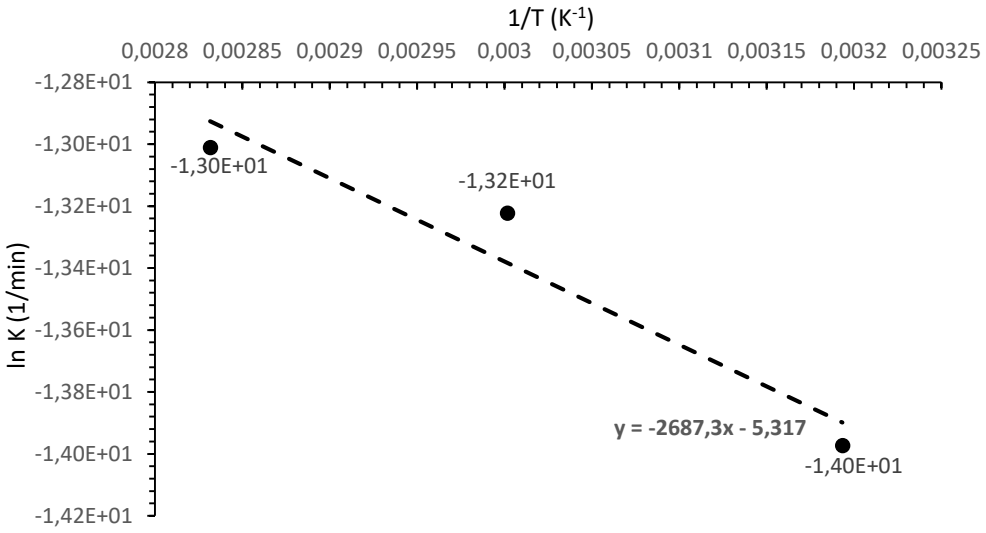

Figure 3.20 *The Arrhenius plot.*

In this way, the linear plot that best fit all the represented points is manifested as the slope the value $-E_a/R$ and as intercept the $ln\,A$. Indeed, if we apply the natural logarithm to both sides to the Equation 3.25, we obtain:

$$\ln K = -\frac{E_a}{R}\frac{1}{T} + \ln A \tag{3.26}$$

That is comparable to the explicit equation of a straight line:

$$y = mx + q \tag{3.27}$$

Where m is the slope while q is the intercept.

The calculated parameters values are reported in **Table *3.7***.

Table 3.7 *Arrhenius parameters.*

$\boldsymbol{A} = 0.004907\ \frac{1}{min}$
$\boldsymbol{E_a} = 22343.48\ \frac{J}{mol}$

Chapter 4

Conclusions and future aims

In summary, during this project, we synthesised and characterised various kinds of manganese based water splitting catalysts that differ in their elemental composition and morphologies. We introduced the use of ionic liquids in the synthesis process as structure directing agents and studied their effect in the resulted materials. Last, with the help of a rapid kinetic study, the parameters as K, A, E_a were calculated and a straight-forward, 1st order kinetic law was modelled.

We have shown how the precipitation method and using ILs can be useful in order to obtain a porous material but, on the other hand, precipitation does not allow for the calcium to intercalate in large amounts inside the structure. Meanwhile, the use of ILs facilitates the aggregation of calcium within the molecular structure, but makes the synthesis process much more expensive especially if the ionic liquid cannot be recovered. We note also how, in many cases, there was a strong presence of carbon in their surface that, as presumably an inert component, inhibits the catalytic power of the sample (it was estimated that with no contamination by carbon, all samples would have been approximately 30% more active).

Thermal treatments have proven to be a mandatory step to increase the porosity and removing contamination rather than raising the percentage of Mn present as Mn(III) that is more active than Mn(II) in the specific case of water-oxidation. The same treatments have also demonstrated to cause a negative effect in case the temperature and time are too elevated because they lead to a crystalline and orderly material (without any defects), contrary to the one observed in the OEC complex.

Experiments on water-oxidation catalysis show a clear difference between samples synthesized through iono-thermal methods and hydro-thermal ones, but above all, they demonstrate that a wide activities can be observed when the different ILs were applied. In particular, we observed as all ionic liquid contained the anion PF_6 have shown to be

insoluble in water, in some way they have a negative effect on the activity (this last aspect has been observed also with anion NTf_2).

The chloride anion seemed as the best choice. Indeed, both samples [Bmim] [Cl] and [N-allyl-HMTA] [Cl] proved to be the most efficient.

Focusing now on these two best performing catalysts, Table 4.1 represents a comparison.

Table 4.1 *Advantages and disadvantages of using the two ionic liquids ([Bmim] [Cl], [N-allyl-HMTA] [Cl]) that lead to the synthesis of the best performing catalysts.*

$[Bmim]^+ Cl^-$	**$[N\text{-allyl-HMTA}]^+ Cl^-$**
1. It is cheaper than [N-allyl-HMTA] Cl. **2.**It is stable up to high temperatures. **3.**To have an appreciable effect on the final material, it's needed in high concentrations (~3.5M). **4.**It is potentially recoverable after its use (by solvent extraction). **5.**Even if present at high concentrations, it does not leave large residues in the final product. **6.**The best annealing parameters contemplate relatively low temperatures (300°C) for a short time (1h) and, thus, this treatment is energetically feasible.	**1.**Its production is more complex than that of [Bmim] Cl. **2.**The degradation temperature is relatively low. **3.**A well performing catalyst is obtained already by using low concentrations (~0.05M). **4.**Because of its degradation at operative conditions, it does not allow for a recovery process (it could be a trouble for its disposal). **5.**Even if it is present as a solvent in really low concentrations, it strongly contaminates the sample which must be annealed. **6.**Because of the high degree of organic contamination, high temperatures are required (500°C).

The table above underline how, even if from the point of view of catalyst activity and ionic liquid concentration needed (during the synthesis) seems better than [N-allyl-HMTA] [Cl]. On the other hand, it can be synthesized more economically

Once the catalyst is chosen, the key factors that make the process more or less economically convenient are mainly two:

1. the make-up (amount) of ionic liquid needed for each synthesis.
2. the lifetime of the catalyst.

During this project, we had not enough time to define design and test any recovery processes for ILs, but in the view of a future scale-up and industrialization, given the high cost of these ionic liquids, we should provide it. However, classic distillation are inefficient in case of these ILs because of the high solubility and strong interactions between water and ILs and so probably the solution could be a solvent extraction (note: distillable ionic liquids exist).

Regarding the lifetime (in the results exposed in 3.3.4) the poisoning effects of cerium ammonium nitrate on catalysts is notable. On the other hand, cerium has been used since it is the perfect oxidising agent for the analysis of activity, thanks to the fact that it does not release oxygen and therefore does not affect the results. However, we have to keep in mind that in an industrial process, changing catalyst every 3-5 hours is not feasible and then we will have to contemplate the use of different oxidant species (like H_2O_2) rather than a classic electrochemical activation of the reaction.

In conclusion, even if the degree of activity obtained was not comparable with the one shown in literature regarding the ruthenium based catalyst, calcium manganese oxide still has a lot of potential to discover. Indeed, remember that unlike ruthenium, elements as calcium and manganese are very cheap and abundant in the earth crust and this is a crucial point if we want to propose a valid alternative to fossil fuels. Furthermore, in a future, by introducing concepts that will help in finding the way of improve these kind of catalysts and solving the troubles met during this project as:

- The porosity of the particles (the 30-40m^2/g obtained, are still low);
- The calcium amount presents within the structure (very low);
- the method with which the catalyst is dropped on the electrode (since an electrochemical way seems to be the best solution for carry on this reaction).

it could be leading to an economically and environmental sustainable pathway to produce oxygen and especially hydrogen for fuel purposes rather than for industrial

supply in order to substitute the current main fossil resources provided by the petrochemicals processes.

Acknowledgements

This project is generously supported by the research team of Prof. Dr. J-PMikkola at the Technical Chemisty, Department of Chemistry, Chemical-Biological Centre, Umeå University. I especially thank the research team for giving me this wonderful opportunity and for their support and availability throughout the work. I also thank all the other collaborators of the research team and not, that in some way they gave their contribution: Phd Tung Ngoc Pham for the B.E.T. analysis and ICP-OES, Dr. Ajaikumar Samikannu for the SEM analysis, Dr. Andras Gorzsas for the Raman spectroscopy and Dr. Andrey Shchukarev for the XPS analysis.

I want also to thank the University of Oulu in Finland, in particular Prof. Krisztian Kordas, M.Sc. Hajimammadov Rashad and then Dr. Sami Saukko (assisting with TEM) and Dr. Marcin Selent (assisting with XRD), both working for the Center of Microscopy and Nanotechnology.

References

[1] Reactions at Surfaces n.d.

[2] Sci C. EDGE ARTICLE Layered manganese oxides for water-oxidation : alkaline earth cations influence catalytic activity in a photosystem II-like fashion † 2012:2330–9. doi:10.1039/c2sc20226c.

[3] https://commons.wikimedia.org/wiki/File:Manganese_cluster_in_the_oxygen-evolving_complex.svg n.d.

[4] Kurz P, Berggren G, Anderlund MF. Oxygen evolving reactions catalysed by synthetic manganese complexes : A systematic screening † 2007:4258–61. doi:10.1039/b710761g.

[5] Mahdi M, Heidari S, Amini E, Khatamian M. Journal of Photochemistry and Photobiology B : Biology Nano-sized layered Mn oxides as promising and biomimetic water oxidizing catalysts for water splitting in artificial photosynthetic systems. J Photochem Photobiol B Biol 2014;133:124–39. doi:10.1016/j.jphotobiol.2014.03.005.

[6] Shinkarev VP, Wraightt CA. Oxygen evolution in photosynthesis: From unicycle to bicycle. Biophysics (Oxf) 1993;90:1834–8.

[7] H. Schiller ‡,§, J. Dittmer ‡, L. Iuzzolino ‡,§, W. Dörner ‡,§, W. Meyer-Klaucke ∥, V. A. Solé ⊥,∇, et al. Structure and Orientation of the Oxygen-Evolving Manganese Complex of Green Algae and Higher Plants Investigated by X-ray Absorption Linear Dichroism Spectroscopy on Oriented Photosystem II Membrane Particles† 1998. doi:10.1021/BI972329B.

[8] Dau H, Grundmeier A, Loja P, Haumann M. On the structure of the manganese complex of photosystem II: extended-range EXAFS data and specific atomic-resolution models for four S-states. Philos Trans R Soc Lond B Biol Sci 2008;363:1237-43-4. doi:10.1098/rstb.2007.2220.

[9] Cox N, Rapatskiy L, Su J-H, Pantazis DA, Sugiura M, Kulik L, et al. Effect of Ca2+/Sr2+ substitution on the electronic structure of the oxygen-evolving complex of photosystem II: a combined multifrequency EPR, 55Mn-ENDOR, and DFT study of the S2 state. J Am Chem Soc 2011;133:3635–48. doi:10.1021/ja110145v.

[10] Sproviero EM, Gascón JA, McEvoy JP, Brudvig GW, Batista VS. A model of the oxygen-evolving center of photosystem II predicted by structural refinement based on EXAFS simulations. J Am Chem Soc 2008;130:6728–30. doi:10.1021/ja801979n.

[11] Takashima T, Hashimoto K, Nakamura R. Inhibition of Charge Disproportionation of MnO_2 Electrocatalysts for Efficient Water Oxidation under Neutral Conditions. J Am Chem Soc 2012;134:18153–6. doi:10.1021/ja306499n.

[12] Cox N, Messinger J. Reflections on substrate water and dioxygen formation.

Biochim Biophys Acta - Bioenerg 2013;1827:1020–30. doi:10.1016/j.bbabio.2013.01.013.

[13] Najafpour MM. Journal of Photochemistry and Photobiology B : Biology Calcium-manganese oxides as structural and functional models for active site in oxygen evolving complex in photosystem II : Lessons from simple models. J Photochem Photobiol B Biol 2011;104:111–7. doi:10.1016/j.jphotobiol.2010.12.009.

[14] C.I. Lee, K.V. Lakshmi, G.W. Brudvig, Probing the functional role of Ca2+ in the oxygen-evolving complex of photosystem II by metal ion inhibition, Biochemistry 46 (2007) 3211–3223. n.d.

[15] T.A. Ono, J.L. Zimmermann, Y. Inoue, A.W. Rutherford, Formation and flashdependent oscillation of the S2 -state multiline EPR signal in an oxygenevolving Photosystem-II preparation lacking the three extrinsic proteins in the oxygen-evolving system n.d.

[16] P. delroth, K. Lindberg, L.E. Andreasson, Studies of Ca2+ binding in spinach photosystem II using45 Ca2+, Biochemistry 34 (1995) 9021–9027. n.d.

[17] Boussac A, Rutherford AW. Nature of the inhibition of the oxygen-evolving enzyme of photosystem II induced by sodium chloride washing and reversed by the addition of calcium(2+) or strontium(2+). Biochemistry 1988;27:3476–83. doi:10.1021/bi00409a052.

[18] Ono T, Rompel A, Mino H, Chiba N. Ca(2+) function in photosynthetic oxygen evolution studied by alkali metal cations substitution. Biophys J 2001;81:1831–40.

[19] Boussac A, Rappaport F, Carrier P, Verbavatz J-M, Gobin R, Kirilovsky D, et al. Biosynthetic Ca2+/Sr2+ Exchange in the Photosystem II Oxygen-evolving Enzyme of Thermosynechococcus elongatus. J Biol Chem 2004;279:22809–19. doi:10.1074/jbc.M401677200.

[20] Grove GN, Brudvig GW. Calcium Binding Studies of Photosystem II Using a Calcium-Selective Electrode †. Biochemistry 1998;37:1532–9. doi:10.1021/bi971356z.

[21] K. Kalosaka, W.F. Beck, G.W. Brudvig, G. Cheniae, Coupling of the PS2 reaction center to the oxygen-evolving center requires a very high affinity Ca2+ site, in: M. Baltscheffsky (Ed.), Current Research in Photosynthesis, Kluwer Academic Publishers, Dordre n.d.

[22] Han K-C, Katoh S. Different binding affinity sites of Ca2+ for reactivation of oxygen evolution in NaCl-washed Photosystem 11 membranes represent differently modified states of a single binding site. Biochim Biophys Acta - Bioenerg 1995;1232:230–6. doi:10.1016/0005-2728(95)00124-7.

[23] Ghanotakis DF, Babcock GT, Yocum CF. Calcium reconstitutes high rates of oxygen evolution in polypeptide depleted Photosystem II preparations. FEBS Lett 1984;167:127–30. doi:10.1016/0014-5793(84)80846-7.

[24] PISTORIUS EK. Effects of Mn2+, Ca2+ and chlorpromazine on photosystem

II of Anacystis nidulans. An attempt to establish a functional relationship of amino acid oxidase to photosystem II. Eur J Biochem 1983;135:217–22. doi:10.1111/j.1432-1033.1983.tb07640.x.

[25] Hoganson CW, Babcock GT. A metalloradical mechanism for the generation of oxygen from water in photosynthesis. Science 1997;277:1953–6.

[26] (a) C.F. Yocum, The calcium and chloride requirements of the O2 evolving complex, Coord. Chem. Rev. 252 (2008) 296–305; (b) J.S. Vrettos, D.A. Stone, G.W. Brudvig, Quantifying the ion selectivity of the Ca2+ site in photosystem II: evidence for direct inv n.d.

[27] Pecoraro VL, Baldwin MJ, Caudle MT, Hsieh W-Y, Law NA. A proposal for water oxidation in photosystem II. Pure Appl Chem 1998;70:925–9. doi:10.1351/pac199870040925.

[28] Limburg J, Szalai VA, Brudvig GW, Debus RJ, Yachandra VK, Sauer K, et al. A mechanistic and structural model for the formation and reactivity of a MnV□O species in photosynthetic water oxidation. J Chem Soc Dalt Trans 1999;1102:1353–62. doi:10.1039/a807583b.

[29] E.M. Sproviero, J.A. Gascon, J.P. McEvoy, G.W. Brudvig, V.S. Batista Computational studies of the O2-evolving complex of photosystem II and biomimetic oxomanganese complexes, Coord. Chem. Rev. 252 (2008) 395–415. n.d.

[30] Jiao F, Frei H. Nanostructured manganese oxide clusters supported on mesoporous silica as efficient oxygen-evolving catalystsw 2010. doi:10.1039/b921820c.

[31] Najafpour MM, Najafpour MM, Ehrenberg T, Wiechen M, Kurz P, Junko Y, et al. Mixed-valence manganese calcium oxides as efficient catalysts for water oxidation. Dalt Trans 2011;40:3793–5. doi:10.1039/C0DT01109F.

[32] R. D. Rogers and K. R. Seddon, Science, 2003, 302, 792–793. n.d.

[33] L. A. Blanchard, D. Hancu, E. J. Beckman and J. F. Brennecke, Nature, 1999, 399, 28–29. n.d.

[34] D. J. Cole-Hamilton, Science, 2003, 299, 1702–1706. n.d.

[35] M. J. Earle, J. Esperanca, M. A. Gilea, J. N. C. Lopes, L. P. N. Rebelo, J. W. Magee, K. R. Seddon and J. A. Widegren, Nature, 2006, 439, 831–834. n.d.

[36] S. L. Chou, J. Z. Wang, J. Z. Sun, D. Wexler, M. Forsyth, H. K. Liu, D. R. MacFarlane and S. X. Dou, Chem. Mater., 2008, 20, 7044–7051. n.d.

[37] A. P. Abbott and K. J. McKenzie, Phys. Chem. Chem. Phys., 2006, 8, 4265–4279. n.d.

[38] W. S. Miao and T. H. Chan, Acc. Chem. Res., 2006, 39, 897–908. n.d.

[39] Morris RE. Ionothermal synthesis — ionic liquids as functional solvents in the preparation of crystalline materials 2009. doi:10.1039/b902611h.

[40] S. J. Mugavero, M. Bharathy, J. McAlum and H. C. zur Loye, Solid State Sci.,

2008, 10, 370–376. n.d.

[41] P. Wasserscheid and T. Welton, Ionic Liquids in Synthesis, Wiley-VCH, Weinheim, Germany, 2003. n.d.

[42] E. R. Cooper, C. D. Andrews, P. S. Wheatley, P. B. Webb, P. Wormald and R. E. Morris, Nature, 2004, 430, 1012–1016. n.d.

[43] Li Z, Jia Z, Luan Y, Mu T. Ionic liquids for synthesis of inorganic nanomaterials. Curr Opin Solid State Mater Sci 2008;12:1–8. doi:10.1016/j.cossms.2009.01.002.

[44] C. S. Cundy and P. A. Cox, Chem. Rev., 2003, 103, 663–701. n.d.

[45] Duan X, Ma J, Zheng W. The art of using ionic liquids in the synthesis of 2014:2550–9. doi:10.1039/c3ce41203b.

[46] H. Ohno, Electrochemical Aspects of Ionic Liquids, Cap 1, John Wiley & Sons, 2011, p. 2005. n.d.

[47] Najafpour MM, Ehrenberg T, Wiechen M, Kurz P. Calcium manganese(III) oxides (CaMn2O4.xH 2O) as biomimetic oxygen-evolving catalysts. Angew Chemie - Int Ed 2010;49:2233–7. doi:10.1002/anie.200906745.

[48] Manual O. Digital Model 10 and Model 20 Controller 2002;44:1–17.

[49] http://hiq.linde-gas.com n.d.

[50] https://www.agilent.com n.d.

[51] http://serc.carleton.edu n.d.

[52] Cleaning S. SEM Sample Preparation Instructions 2008:7–8.

[53] Sing K. The use of nitrogen adsorption for the characterisation of porous materials 2001;188:3–9.

[54] K.S.W. Sing et al., Pure Appl. Chem. 57 (1985) 603. n.d.

[55] S.J. Gregg, K.S.W. Sing, Adsorption, Surface Area and Porosity, Academic Press, London, 1982. n.d.

[56] J. Roquerol, F. Rodriguez-Reinoso, K.S.W. Sing, K.K. Unger (Eds.), Characterization of Porous Solids III, Elsevier, Amsterdam, 1994. n.d.

[57] F. Rodriguez-Reinoso, J. Roquerol, K.S.W. Sing, K.K. Unger (Eds.), Characterization of Porous Solids II, Elsevier, Amsterdam, 1991. n.d.

[58] K.K. Unger, J. Roquerol, K.S.W. Sing, H. Kral (Eds.), Characterization of Porous Solids, Elsevier, Amsterdam, 1988. n.d.

[59] Leofanti G, Padovan M, Tozzola G, Venturelli B. Surface area and pore texture of catalysts. Catal Today 1998;41:207–19. doi:10.1016/S0920-5861(98)00050-9.

[60] Micromeritics. TriStar 3000 Manual. vol. 8. 2007.

[61] http://xpssimplified.com n.d.

[62] http://ruby.chemie.uni-freiburg.de/Vorlesung/methoden_I_7.xhtml n.d.

[63] C. Chen, G. Ding, D. Zhang, Z. Jiao, M. Wu, C. -H. Shek, C. M. Lawrence Wu, J. K. L. Lai and Z. Chen, Nanoscale, 2012, 4, 2590–2596. n.d.